

UCRL-JC- 118317  
PREPRINT

**Characterization of Waste Drums  
Using Nonintrusive Active and Passive  
Computed Tomography**

**G. P. Roberson, H. E. Martz, D. J. Deckman,  
D. C. Camp, S. G. Azevedo and E. R. Keto**

**This paper was prepared for submittal to  
Nondestructive Assay & Nondestructive Examination  
Waste Characterization Conference  
Pocatello, Idaho  
February 14-16, 1994**

**August, 1994**

**This is a preprint of a paper intended for publication in a journal or proceedings. Since changes may be made before publication, this preprint is made available with the understanding that it will not be cited or reproduced without the permission of the author.**

**MASTER**

The logo for Lawrence Livermore National Laboratory, featuring a stylized 'L' symbol and the text 'Lawrence Livermore National Laboratory' arranged in a triangular shape.

**Lawrence  
Livermore  
National  
Laboratory**

#### DISCLAIMER

This document was prepared as an account of work sponsored by an agency of the United States Government. Neither the United States Government nor the University of California nor any of their employees, makes any warranty, express or implied, or assumes any legal liability or responsibility for the accuracy, completeness, or usefulness of any information, apparatus, product, or process disclosed, or represents that its use would not infringe privately owned rights. Reference herein to any specific commercial products, process, or service by trade name, trademark, manufacturer, or otherwise, does not necessarily constitute or imply its endorsement, recommendation, or favoring by the United States Government or the University of California. The views and opinions of authors expressed herein do not necessarily state or reflect those of the United States Government thereof, and shall not be used for advertising or product endorsement purposes.

## **DISCLAIMER**

**Portions of this document may be illegible in electronic image products. Images are produced from the best available original document.**

# CHARACTERIZATION OF WASTE DRUMS USING NONINTRUSIVE ACTIVE AND PASSIVE COMPUTED TOMOGRAPHY

G. Patrick Roberson, Harry E. Martz, Daniel J. Decman, David C. Camp  
Steven G. Azevedo and Eric R. Keto

Lawrence Livermore National Laboratory  
Livermore, CA 94551, USA

## ABSTRACT

We have developed a data acquisition scanner for gamma-ray nondestructive assay (NDA) active and passive computed tomography (A&PCT) along with associated computational techniques for image reconstruction, analysis, and display. We are using this scanner to acquire data sets of mock-waste drums at Lawrence Livermore National Laboratory (LLNL). In this paper, we discuss some issues associated with gamma-ray spectroscopy assay, NDA imaging, describe the design and construction of an NDA drum scanner and report on code development for image reconstruction. We also present representative A&PCT assay results of well characterized mock-waste drums. These preliminary results suggest that A&PCT imaging can be used to produce accurate absolute assays of radioactivity in real-waste drums.

## I. INTRODUCTION

Characterization of mixed (radioactive and hazardous) wastes requires that the identity and strengths of intrinsic radioactive sources be determined accurately and that all hazardous (e.g., heavy metals, volatile organic compounds—VOCs—and non-VOCs) and non-conforming materials (e.g. free liquids, sharp objects, particulates, and pressurized containers) be identified.[AND91] We are developing both nondestructive evaluation (NDE) and assay (NDA) methods to meet some of these characterization requirements. The NDE methods include x-ray real-time radiography (RTR), digital radiography (DR), and transmission computed tomography (TCT), while the NDA method is gamma-ray active (A) and passive (P) computed tomography (CT). Here we describe only the NDA waste-drum characterization research and development (R&D) activities at the Lawrence Livermore National Laboratory (LLNL). Our NDE activities are described elsewhere in these proceedings.[MAR94]

Current practice within DOE for characterizing nuclear wastes include two nondestructive assay (NDA) techniques. Passive and active neutron (PAN) interrogation is an NDA method that determines the amount of spontaneous (passive) and induced (active) fissionable isotopes present.[CAL86] Segmented gamma-ray spectrometry (SGS) is an NDA method that measures the amount of only  $^{235}\text{U}$  or  $^{239}\text{Pu}$  in a waste drum.[SIM90] It is important to emphasize that these techniques were not developed to assay unknown wastes but rather to measure large amounts (on the order of grams) of special nuclear materials given prior knowledge of the radioactive isotopes. Furthermore, these techniques are applicable only under the assumption that the radioactive sources are uniformly distributed in a uniformly attenuating matrix. This is typically not the case for real wastes. Thus we have been developing a gamma-ray computed tomography technique to resolve some of these inconsistencies to better assay a waste drum. This new gamma-ray CT technique is called active and passive CT (A&PCT).

MASTER



The operating principle of the A&PCT technology is quite simple. Two measurements are required; an active and a passive computed tomography measurement. The active computed tomography (ACT) measurement maps an unknown drum's waste matrix as a function of gamma-ray energy. The passive computed tomography (PCT) measurement identifies and localizes all of the radioisotopes detected. Finally, by combining the PCT measurements with the ACT measurements, we are able to correct all of the measured, passive gamma-ray intensities for drum-content attenuation. The corrected passive gamma-ray intensities provide a quantitative measure of the source strength of all detected internal radionuclides; hence, enable us to classify detected radioactivities within the drum as transuranic or low-level according to their measured activities and to repository regulations. In addition to our efforts, at least six other groups—two within the US, [BER94 & EST90] two in Japan, [KAW90 & GOT91], one in Germany [REI92] and one in Hungary [LEV94]—are investigating NDA techniques that are either directly or indirectly based on standard A&PCT methods. Some of our preliminary A&PCT results have been presented elsewhere.[CAM92, MAR92, MAR92a, MAR92b, MAR91 and MAR90]

We report here on the gamma-ray A&PCT scanner developed and our results for the assay of mock wastes. Before describing the scanner and results in detail we present a brief section description of the principles and issues related to the assay of 208-liter waste drums.

## II. BACKGROUND

There are three distinct components to the assay of an unknown waste drum using gamma-ray active and passive CT. These components are (1) gamma-ray spectroscopy; (2) A&PCT data acquisition; and (3) active and passive image reconstruction. We briefly describe the principles and issues associated with each of these to better understand the challenge of the nondestructive assay of waste drums.

### Gamma-ray spectroscopy for radioactive assay

Gamma-ray spectroscopy with high-spectral resolution germanium detectors has been successfully used as a quantitative radioactive assay method for many years.[DEB88] The high-spectral resolution allows for confident radionuclide identification. The high-spectral resolution also increases the signal-to-noise ratio enabling precise measurement of the line strengths (peak areas) in complicated spectra. Gamma-ray spectroscopy applied to radioactive waste drums involves additional complications. These include the possibly large size of the sources and the attenuation of radiation by drum contents. For small (point) sources, several methods accurately relate line strengths to absolute assay values. For sources that are roughly the size of the detector area, there are methods to extend the point source calibration to yield an absolute assay. These methods become less reliable as the source dimensions become much larger than the detector.[DEB88] Sources in 208-liter drums are much larger than the 45 cm<sup>2</sup> detector area.

This problem is made even more complicated by attenuation. Conventional gamma ray spectroscopy methods can account for attenuation if the source is uniformly distributed in a homogeneous attenuating matrix. Real-waste drums rarely meet either of these conditions.

An example of a conventional gamma-ray spectroscopy method that has been applied to assay waste drums is the Los Alamos National Laboratory (LANL) segmented gamma-ray spectrometer (SGS).[SIM90] The SGS technique is DOE's current state-of-practice in measuring gamma-rays from contained radioactive wastes. This technique is often inaccurate because waste drums rarely conform to the assumptions of conventional gamma-ray spectrometry.

Quoted precisions obtained for SGS assays of weapons grade (WG) Pu in 208-L drums are  $\pm 100\%$  for  $\leq 1\text{g}$ ,  $\pm 10\%$  for  $10\text{g}$ , and  $\pm 3\%$  for  $30\text{g}$ . The maximum allowable WG Pu content in a drum differs, but must be  $< 200\text{g}$  to meet WIPP disposal requirements. For a 208-L drum containing  $100\text{ kg}$  of wastes, only  $160\text{ milligrams}$  of  $^{239}\text{Pu}$  are required to shift the drum from the LLW to the TRU category. SGS is not capable of making an accurate assay for this small amount of WG Pu. Thus, SGS cannot satisfy current regulations.

The reason for SGS's inaccuracy is poor spatial resolution. Therefore we are developing a more refined technique that improves the resolution from a few large segments ( $\sim 20\text{ cm}$  high by  $\sim 60 \times 60\text{-cm}$  square) used in SGS to many small (from  $1.27$  to  $5\text{ cm}$  on a side) volume elements or voxels. Our system over comes the limitations of conventional gamma-ray spectroscopy. We can accurately use point source calibration data because our voxels are small. Our system uses active computed tomography (ACT) to measure the attenuation for each voxel and corrects the line strengths to obtain accurate identifications and assays.

#### A&PCT data acquisition

Our A&PCT scanner acquires two data sets ACT and PCT separately. The quantity that is reconstructed in ACT is the attenuation value at a particular photon energy for some voxel at location  $x,y,z$  within the drum. The attenuation due to the drum's contents, whether heterogeneous or homogeneous, is accurately measured in all three dimensions of the drum. It is useful to note that a single ACT measurement at a single energy is analogous to a simple gamma-ray transmission gauge. By measuring the attenuation at several energies one can determine the attenuation correction for any of the energies matching any isotope line measured by PCT.

PCT measures the presence and identity of an emitting radioisotope(s). The ray sum for passive or single-photon-emitted CT (sometimes called SPECT) is the integrated activity over the path length of the passive source(s) within the waste drum attenuated by any absorbers along the path. The contents of the drum are usually unknown but the attenuation may be large and not homogeneous. Our system uses ACT to determine the structure of absorbers and correct the PCT data for attenuation.

The PCT spectroscopy identifies a broad range of isotopes. Our PCT system collects data over a wide range of energies at high-spectral resolution ( $\sim 1\%$ ). Using this data and LLNL isotope gamma-ray spectroscopy codes isotopes are readily identified by their spectral signature. This provides an accurate determination of the activities for all detected radioisotopic sources.

#### A&PCT image reconstruction

Image reconstruction is the task of determining the structure of an object voxel by voxel from its projections or ray sum data. For our A&PCT system the reconstruction proceeds in two steps. The first produces a map of the attenuation from the active data; the second uses passive ray sum data to localize the sources of radioactivity and the active data to correct the radioactivity for attenuation to determine the absolute assay. The reconstruction of an attenuation map from the active, or transmission, data has been extensively developed and there are several excellent algorithms. We use filtered backprojection a standard in industry.[MAR92c & ROB92] The real challenge for A&PCT comes in the second step.

Several factors conspire to make PCT image reconstruction significantly more complex than ACT. First the position of the source(s) are initially unknown. Unlike ACT where the active source is a fixed distance from the detector, in PCT the  $1\text{ over }r^2$  decrease in photon flux cannot be determined in advance. Similarly because the source positions are unknown, it is not possible to correct the source strengths for attenuation independently of the reconstruction. Both these effects must be accounted for simultaneously with the

reconstruction itself. Secondly in PCT, the ray sum data is acquired with the use of collimators. Unlike ACT where the ray paths are simply defined by the line from the active source to the detector, in PCT the emission is integrated over a diverging cone of acceptance whose width increases linearly with distance away from the detector. A PCT reconstruction algorithm must account for this spatially dependent instrument response. Thirdly in PCT, the number of collected photons is dependent on the activity within the drum. Unlike ACT where the active source can be made intense, in PCT the number of collected photons could be quite low. Poor counting statistics affect both the accuracy and the robustness of image reconstruction. Thus a PCT algorithm must be forgiving of noisy data.

Although passive tomography is not a new field, most reconstruction algorithms do not fully account for these effects and therefore are not accurate. In medical imaging, these effects while present are not as severe and approximate corrections are used. These approximations may result in qualitatively faithful images with poor quantitative accuracy.

We are working with the University of California at San Francisco (UCSF) to develop a reconstruction procedure that accounts for these effects. In our approach, called MLEM (Maximum Likelihood-Expectation Maximization), we consider the data to be the result of a stochastic process based on a Poisson probability distribution. For any given model of the source, there is a certain probability of actually obtaining the measured data. In the reconstruction the model of the source is varied to maximize the probability of obtaining the measured data.[BRO92] Our present procedure handles 2D images—it assumes that the source structure is uniform along one axis (line sources). We are working with UCSF to develop a 3D image reconstruction program that makes no assumptions as to source structure.

### III. A&PCT SCANNER DESCRIPTION

For research and development of the assay of 208-L nuclear waste drums, we have designed and constructed an A&PCT prototype scanner. The A&PCT scanner is a first generation (translate/rotate), nuclear-spectroscopy based system. Figure 1 shows this type of scanner and two other different scan modes used in computed tomography. Although this prototype scanner implements a single-discrete detector, first-generation scanning mode, nuclear-spectroscopy based systems including the A&PCT scanner, do not necessarily have to be performed in a first-generation data-acquisition mode. Multiple detectors arranged in a linear or area-array can acquire nuclear-spectroscopy data much faster in second- and possibly third-generation modes of acquisition. Once A&PCT is proven to be able to accurately assay waste drums using a single detector scanner, it is fairly straight forward to design and construct a multi-detector-based scanner to more rapidly assay waste drums.

The scanner components include an energy-discriminating detector, spectroscopy electronics, a gamma-ray source, a three-axis (translate, elevate, and rotate) drum manipulator and computers for data acquisition, control, image reconstruction and analysis. The source and detector are both collimated. Figure 2 is a block diagram of the prototype scanner. Figure 3 is an engineering drawing of the A&PCT prototype scanner showing the position of the gamma-ray source, drum manipulator and energy-discriminating high purity germanium (HPGe) detector. The prototype scanner is located at Lawrence Livermore National Laboratory's Site-300 facility. The scanner is shown in the photograph of Figure 4. Both the drawing and photograph show that the drum manipulator is located in a pit that provides room for the stage and therefore keeps the source and detector subsystems low to the ground. Also shown in the photograph is a large lead (Pb) wall between the drum manipulator and the detector system. The wall has a hole or window that allows the detector to view the waste drum. This wall shields the detector from radioisotope sources within the drum except through the aperture of the detector collimator. The A&PCT

prototype system is constructed of clamping rails that provide the flexibility to reconfigure the external framework and conduct a variety of experiments to best understand the trade offs among the multitude of CT data acquisition parameters.

#### A&PCT detector system

The A&PCT scanner uses an intrinsic high-purity Germanium detector and nuclear-spectroscopy electronics to acquire gamma-ray spectra from either the active source and/or any detectable gamma rays for passive sources emitting from within the waste drum. The configuration of the detector and spectroscopy electronics is shown in Figure 5. An IBM computer is used for data acquisition and stage control. The detector has a relative efficiency of 90% with an energy resolution (FWHM) of 1.73 keV at 1.33 MeV. High-detector efficiency is desired for imaging low-intensity radioisotope sources and high-energy resolution is required to accurately identify all detected radioisotope sources that may be within the waste drums.

#### Three axis drum manipulator

The A&PCT prototype scanner contains a three-axis manipulator that translates, elevates and rotates the waste drum under observation. Three axes of freedom are necessary for first-generation CT scan mode data acquisition. The A&PCT prototype first-generation scanner requires that the drum be translated along the horizontal axis in discrete steps or continues motion. At each step or sampling point, line integrals (also called ray sums) are collected by the nuclear-spectroscopy detector electronics. A set of line integrals for a full translation of the drum is required and is called a projection. The reconstruction algorithms require that line integrals be acquired for many angles around the object, therefore, after each projection is acquired, the drum is rotated slightly and another set of line integrals are collected. From these line integrals, the attenuation value or the passive source intensity for some voxel, at location  $x,y,z$  within the drum is calculated. By translating the drum in the vertical axis, the attenuation values or the passive source intensities can be measured in the third dimension at different  $z$  planes (or elevations) of the drum.

#### A&PCT prototype Gamma-ray active sources

The A&PCT radioisotopic active source produces gamma-rays using either  $^{192}\text{Ir}$  (with major peaks at 296, 308, 317, 468, and 604 keV) or  $^{166\text{m}}\text{Ho}$  mixed with  $^{60}\text{Co}$  (with major peaks at 184, 281, 365, 411, 530, 712, 810, 951, 1173 and 1332 keV). Figure 6 shows a sample of the data acquired from each radioisotopic active source after attenuation by the waste drum. Several major peaks for each isotopic source are identified in the figure. The  $^{166\text{m}}\text{Ho}$  source is a new upgrade to the LLNL prototype A&PCT scanner and is a preferred active source over the  $^{192}\text{Ir}$  source. Since the  $^{166\text{m}}\text{Ho}$  source is rather unique, we describe its irradiation and fabrication below.

#### *$^{166\text{m}}\text{Ho}$ Gamma-Ray active source*

The  $^{166\text{m}}\text{Ho}$  has a 1200-year half-life, which means that no half-life corrections need to be applied for data acquired over weeks of time. The radioisotope emits many strong gamma rays that, fortunately, decrease in intensity almost monotonically with increasing energy. When the  $^{166\text{m}}\text{Ho}$  gamma rays are transmitted through the waste drum, the lower-energy gamma rays are attenuated more strongly, while the higher-energy gamma rays suffer less attenuation for the detector used in the prototype scanner. The result is that for the most common waste densities, that range from 0.5 to 1.5 g/cm<sup>3</sup>, the emitted  $^{166\text{m}}\text{Ho}$  gamma rays emerge from the waste drum with nearly the same intensities detected in the HPGe detector, regardless of energy. This source coupled with the emitted gamma

rays from  $^{60}\text{Co}$  provide nine intense monoenergetic, transmitted energy regions-of-interest (EOIs) from 184 keV to 1.33 MeV with an average energy separation of 145 keV. These EOIs can be used to construct nine separate monoenergetic attenuations maps of the waste matrix that are useful in the correction of passively measured CT data.

#### *$^{166}\text{mHo}$ Source Irradiation and Fabrication*

Holmium oxide was purchased from Rhone-Poulenc, In., Phoenix, AZ. The purity was specified by the manufacturer as 99.999% holmium oxide. Inductively coupled plasma - atomic emission spectroscopy was performed on the holmium oxide at LLNL. A few other rare earths were found, primarily in the few ppm trace range, however, none resulted in any significantly intense gamma-ray emissions.

Ten grams of holmium oxide was sent to the High Flux Irradiation Facility (HFIR) at the Oak Ridge National Laboratory (ORNL) for irradiation. Typical irradiation time was 3 days in one of the central core positions, which had a neutron flux of  $1.6 \times 10^{15}$  n/cm<sup>2</sup>/sec. The holmium oxide was loaded by HFIR personnel into 2.54-cm long, high-purity aluminum tubes with a 0.65 cm outer diameter with a wall thickness of 0.4 mm. About 160 milligrams of holmium oxide were loaded into each aluminum tube, covered (top and bottom) with high-purity aluminum powder, and pressed at  $4.0 \times 10^8$  Pa (60,000 lbs/in<sup>2</sup>). This compression resulted in a cold-weld aluminum capsule with a 0.65-cm outer diameter and 1.3-cm long. Irradiation in HFIR resulted in an activity that averaged 1.08 mCi/mg, or about 177  $\mu\text{Ci}$  per capsule.

A total of 51 such capsules were irradiated in HFIR and the least distorted and mechanically sound capsules (48 in all) were used to make six,  $2.7 \times 2.7$ -cm sources. Each capsule was calibrated on the same HPGe spectrometry system at the same fixed distance, and each capsule's specific activity was measured individually to an accuracy of 2%. After counting all the irradiated capsules, they were selected to create six, 8-capsule sources having very nearly the same specific activity. The individual capsules were loaded into a  $2.7 \times 2.7$ -cm  $\times$  1.3-cm thick, Lucite holder with four 0.66-cm diameter holes drilled to within 0.6-mm of its bottom and separated by 0.235 mm (bottom left Figure 7). Into each of the four holes, two capsules were stacked, one on top of the other. Each square,  $^{166}\text{mHo}$  source had a mean activity of 1.42 mCi with a variation of only 0.08 mCi. The following is a table showing the activity of each of the six sources.

Table 1 Total Activity of each of the six square sources

Source	$^{166}\text{mHo}$ (mCi)	$^{60}\text{Co}$ ( $\mu\text{Ci}$ )
A	1.450	215
B	1.420	208
C	1.455	210
D	1.420	195
E	1.400	220
F	1.370	204

The high-purity aluminum used to encapsulate the holmium oxide has a few parts per million transition metal impurities. Upon irradiation in the HFIR, these impurities produced several short-lived radioisotopes, specifically,  $^{59}\text{Fe}$ ,  $^{46}\text{Sc}$ ,  $^{54}\text{Mn}$  and  $^{60}\text{Co}$ . The  $^{60}\text{Co}$  is a desirable activity since it emits two, very intense gamma rays at 1.173 and 1.3325 Mev. It has a half-life of 5.272 years, so it becomes, along with the 1200-yr half-life  $^{166}\text{mHo}$ , a source of gamma rays for ACT measurement. The mean specific



activity of the  $^{60}\text{Co}$  in the six, 8-capsule sources was 0.209 mCi with a maximum variation of 0.035 mCi.

#### *$^{166}\text{mHo}$ Source holder and Irradiation Shield*

A relatively simple radiation source holder and personnel radiation shield was constructed using machined lead bricks enclosed in a welded stainless-steel box. The box has two stainless steel handles on either side to enable two people to handle the 73 kg source holder. The enclosure was made from 0.64-cm stainless steel, and measured 25.4-cm long, 15.24-cm wide, and 12.7-cm high and is shown in the simplified diagram on the right of Figure 7. In the center of a standard 20.23-cm long, by 10.16-cm wide, by 5.08-cm thick lead brick, a 1.9-cm deep by 2.54-cm wide channel was machined from the front of the brick to within 2.54 cm of the back of the brick. This brick served as part of the bottom of the shield. In a second standard lead brick, a 0.635-cm deep by 2.54-cm wide channel was machined to match the channel of similar dimensions in the bottom brick. These two bricks form the top and bottom of the 2.54-cm square aperture  $^{166}\text{mHo}$  active source holder and collimator. Three additional 2.57 by 2.57-cm slots were machined in the top and bottom lead bricks beginning at 5.08-, 10.16- and 15.24-cm respectively, from the front of the brick housing. The slots are slightly wider than 2.54-cm and hold two of the 2.7-cm  $\times$  2.7-cm  $\times$  1.26-cm plastic  $^{166}\text{mHo}$  source holders shown on the bottom left of Figure 7. Along the sides of both the top and bottom bricks, a 0.635-cm step was machined. When the top brick is placed on the bottom brick, no source irradiations can escape through this step-wise closure. Additional standard lead bricks were appropriately machined and placed to the rear and on top of these two central lead bricks, thereby filling the entire 25.4-cm long, 15.24-cm wide, and 12.7-cm high enclosure with lead for additional shielding.

#### Acquisition, control, reconstruction and analysis computers

The A&PCT scanner uses an IBM computer to control the three axis drum manipulator and acquire the spectroscopy data. The IBM computer is connected to the three axis stage controller via a RS-232 serial port. All commands to control the staging system are sent over the serial port. Also, the position of the stage can be polled from the controller through the serial port. The position of the staging system is recorded on the hard disk of the computer after each move so that if power is lost, and the A&PCT experiment is halted, the experiment can be restarted at the last position acquired.

For spectroscopy data acquisition, the IBM is connected to a multichannel buffer via a parallel port. The scanner can acquire an entire spectrum at each integration point, or extract the number of photons detected over several energy regions-of-interest thus the data is acquired at several specific energies simultaneously. After acquisition, the data is transferred to a UNIX based computer systems for data preprocessing, image reconstruction and analysis. This transfer is made via a network connection or by floppy disk.

#### The A&PCT prototype collimators

The spatial resolution for both the active and passive images produced by the A&PCT prototype scanner is defined by the step size taken for each integration point and the collimator aperture size. The prototype scanner has three sets of fixed, square-aperture collimators with aperture sizes of  $1.27 \times 1.27$ ,  $2.54 \times 2.54$ , and  $5.08 \times 5.08$  centimeters. Each set contains three collimators, one for the source and two for the detector. All collimators are 12.7-cm long with the exception of the  $^{166}\text{mHo}$  active source collimator. The  $^{166}\text{mHo}$  source holder has a built-in collimator with a square 2.54-cm aperture that is 5.08-cm long.

The detector collimation system consists of three parts, a large lead wall, and two small collimators. One of the small collimators (the wall collimator) is at the front of the lead wall (the source side) and the other (the detector collimator) is just in front of the detector as shown in the engineering drawing of Figure 8. The lead wall is extremely heavy and would be difficult to align to the other scanner components, therefore, the detector viewing window within the lead wall is made large compared to the desired aperture size, and the two smaller collimators are used for alignment. The wall and detector collimators provides the A&PCT prototype scanner with the ability to adjust the aspect ratio. The collimator aspect ratio is defined as the length of the overall collimator to the size of the aperture opening. The aspect ratio affects the system response and thus the final assay accuracy. The length of the detector collimator is measured from the front (source side) of the wall collimator to the the end (detector side) of the detector collimator. As shown in Figure 8, the length of the detector collimator is adjustable by moving the small detector collimator and detector towards or away from the lead wall. The largest aspect ratios that can be achieved are 20:1, 40:1 and 80:1 for the 5.08-, 2.54- and 1.27-cm aperture collimators, respectfully. Also, the small detector collimator can be removed from the scanner frame and the detector can be moved forward into the lead wall viewing window. This provides the smallest aspect ratio possible, i.e. 2.5:1, 5:1 and 10:1 for the 5.08-, 2.54- and 1.27-cm aperture collimators, respectfully.

#### IV. EXPERIMENTS, RESULTS AND DISCUSSION

We have performed a series of experiments to demonstrate the performance of the A&PCT method in characterizing radioactive waste drums. Our first experiments focussed on the ability to correct the passively measured data with an ACT attenuation map. These experiments included a reference PCT scan acquired with only the passive CT source, i.e. there is no attenuation of the source by the drum or it's contents. The passive measurements that were obtained by these same sources attenuated by a 208-L drum and mock-waste matrix is then compared to the reference scan. Thus the success of the preliminary measurements was not the agreement of an absolute assay with the known activity of the sources but rather how well we could correct for attenuation by the drum and waste matrix. This was determined by comparing the corrected PCT image to the reference scan. Our results were successful and are described below.

Since the above experiments show that we can correct for the mock-waste attenuating matrix we are currently developing a method for absolute assay determination. A second set of measurements were obtained to study the UCSF MLEM absolute assay method and acted as a test of the reconstruction code.[BRO92] These measurements were performed with a calibrated  $^{133}\text{Ba}$  passive source and either a simple uniform attenuator (aluminum cylinder) or a mock waste drum. All of these experiments are described below.

All active CT measurements were performed using either an external  $^{192}\text{Ir}$  or  $^{166}\text{Ho}$  source. For this application we used the 317-keV transition of  $^{192}\text{Ir}$  and the 365-keV transition of the  $^{166}\text{Ho}$  source to map the attenuation of the waste matrix that is used to correct the 356-keV transition of the  $^{133}\text{Ba}$  passive source. In the active measurements the drum or Al cylinder was translated in 27, 2.54-cm steps through the source-detector plane and the photon spectrum was measured. These translations were performed for each of 40 object rotations over 180 degrees. The active data were reconstructed to form an attenuation map for that particular section of the drum or cylinder. This map is used to correct the passive CT data. A program of translations and rotations, similar to the active CT measurement, was again performed without the external active source to create the passive CT data sets.

The active CT data are displayed as pixel values that represent the attenuation for a  $2.54 \times 2.54 \times 2.54$ -cm volume cube within the aluminum cylinder or waste drum. There are several ways to qualitatively and quantitatively analyze the active data. The easiest is to visually or qualitatively compare the gamma-ray attenuation coefficient fluctuations within each image and from image to image. This technique can be used to spot gross anomalies within an image and to compare one image to the next. A gray scale or color scale/color bar can be used to quantitatively compare the change in attenuation within each image and from image to image. The passive CT data are displayed as pixel values that represent the peak area or branch activity of the radioisotopes of a  $2.54 \times 2.54 \times 2.54$ -cm volume cube within the Al cylinder or waste drum. Similar to the active data, a gray scale or color scale/color bar can be used to quantitatively compare a change in the peak area activity of the passive source within each image and from image to image.

#### First mock waste drum experiments using reference data

Active and passive scans were acquired on a 208-liter drum with mock wastes and a radioactive passive source to determine what the nondestructive A&PCT technology could reveal about the contents of a closed container. The mock waste consisted of three plastic bags filled with paper, glass, and metal, respectively as shown in Figure 9. These bags were placed inside the drum at approximately the same height on a divider shelf that is fastened to the drum wall. A  $^{133}\text{Ba}$  radioisotope sealed source was used to represent the passive radioactive source inside the drum. This source was positioned between the glass and metal bags. The  $^{133}\text{Ba}$  source was fastened to a pedestal that was secured to the rotational stage of the scanner.

Three aluminum tubes penetrate the mock waste drum and allow radioactive sources that represent radioactive waste to be inserted at any depth within the drum without obstruction from the waste matrix. This allows us to measure the performance of the A&PCT technique to assay a drum with heterogeneous waste contents. One tube is positioned at the center axis of the drum, one is positioned adjacent to the drum perimeter and the last tube is positioned midway between the first two tubes. For this experiment, the drum was positioned over the passive source and pedestal so that the source would enter the tube between the drum center axis and outer edge.

A series of data sets have been acquired using different integration times. Each set consists of two passive and one active scan. Of the passive scans, one is used as a reference (without drum or waste as attenuators). The second passive scan and the active scan were obtained on the drum at the same location with mock waste and the passive  $^{133}\text{Ba}$  source. For the active scan, the 317-keV transition of the  $^{192}\text{Ir}$  external gamma-ray source was used. Both the active and passive data sets were acquired using an integration time of 150 and 1.5 seconds per ray sum for the data presented here.

These data sets are being used to investigate: (1) ACT to obtain images that represent cross-sectional attenuation maps of a waste-canister's contents; (2) PCT to locate and determine the identity of any radioisotopic source(s) present; and (3) ACT data to correct the PCT data so that accurate source strengths can be determined.

Representative A&PCT results are shown in Figure 10 for the 150 second integration time and Figure 11 for the 1.5 second integration time. One useful form of data analysis is to compare the summed peak area activity value of the reference PCT images (Figures 10b and 11b) to the summed peak area activity value of both the non attenuated and attenuated (corrected) PCT images (Figure 10c&d and 11c&d). The results of this comparison reveals that the uncorrected PCT (Figure 10c and 11c) summed peak area activity values for both data sets are approximately 43-45% lower than the reference values. This is as expected, since we do not account for the attenuation by the drum and mock-waste matrix. The PCT images that are corrected for attenuation (Figure 10d and 11d) yields a summed activity value approximately 10% higher than the reference value in both cases. The



attenuation corrected PCT summed activity value is closer to the reference value, as we would expect. However, it is not clear why it is overcorrected by ~10%. This error is most likely due to the assumption of a non diverging detector collimator geometry for passive data acquisition. These were corrected for attenuation and reconstructed using a WLS/SD code developed by Donner Lab.[HUE77 & ROB92]

These preliminary 208-l A&PCT scan results reveal that PCT can localize and identify the internal radioactive isotopes; and ACT scans properly map the canister's attenuating matrix such that, when coupled with PCT scans, they yield more accurate passive source activity values. A comparison between the 150 and 1.5 second data sets reveal that reducing the data acquisition time by a factor of 100 apparently has little effect on the accuracy of the assay. Future evaluation of the data acquisition time parameter is left for future work.

#### Absolute measurement with uniform attenuation

An aluminum cylinder was used as a uniform attenuator to evaluate the active and passive image reconstruction algorithms. This experiment was conducted to evaluate the algorithms ability to perform an absolute activity measurement of the  $^{133}\text{Ba}$  source when correcting for the attenuation caused by the aluminum cylinder. The cylinder was used to create a simplified passive CT data set with uniformly attenuated ray sums. A diagram of the cylinder is shown in Figure 12. The cylinder is 7.62-cm high with a 20.32-cm outer diameter and 5.05-cm wall thickness. The  $^{133}\text{Ba}$  passive source was placed in the center of the aluminum cylinder. The 356-keV transition of the  $^{133}\text{Ba}$  source was attenuated approximately 70% by the 5.05-cm aluminum wall of the cylinder. Data was acquired for 100 seconds for each ray sum. The 365-keV transition of the  $^{166}\text{Ho}$  active source was used to correct the passive data set.

The active and passive data reconstructions were performed using a new code developed by UCSF that accounts for the non-parallel geometry (diverging detector acceptance angle) of our CT measurement system. It is important to note that the code used in this work accounts only for the geometrical effects in the translational direction. This 2D code assumes a line source geometry for the emitting object to calculate the vertical effect. For the point source data considered here, we are able to correct for this source shape assumption. The analysis of more complicated source geometries requires a true 3D code. Such a code is currently under development.

Only two measurements were required for this absolute assay experiment, one active scan and one attenuated passive scan. Both active and passive scans were performed on the central section of the aluminum cylinder where the  $^{133}\text{Ba}$  source was placed. No reference data was acquired for this experiment because an absolute measurement was the desired result. Figure 13 summarizes the results for this experiment. Figure 13a is the reconstructed active image that was obtained from the 365-keV transition of the  $^{166}\text{mHo}$  source. This attenuation map shows pixels with values that represent the attenuation coefficient in inverse centimeters. The color bar above the attenuation map shows the higher attenuating items are represented by white to gray, and low attenuating items are represented by gray to black. Figure 13b is the uncorrected passive image of the 356-keV transition of the  $^{133}\text{Ba}$  source and Figure 13c is the attenuation corrected passive image. The location of the  $^{133}\text{Ba}$  passive source within the active attenuation map is shown in Figure 13a. The corrected passive image was summed to yield a corrected source peak area activity of  $57.9 \times 10^6$  counts. Correcting these photon counts for the 356-keV branching ratio of the  $^{133}\text{Ba}$  passive source, and detector efficiency, the source assay value was determined to be 75  $\mu\text{Ci}$ . This value is within 8.5% of the actual (or ideal) value of the  $^{133}\text{Ba}$  source on the date the experiment was performed.

### Well characterized TRU/LLW drum experiments

In addition to the above experiments, we have successfully scanned a well characterized mock-waste (standard) drum containing representative low-level waste (LLW) and transuranic (TRU) waste items using the A&PCT assay method. A diagram and photograph of the waste drum is shown in Figure 14. The mock-waste drum is a standard 208-liter (55-gallon) steel drum with a 0.1 mm thick plastic bag used as an inner liner that encloses the entire content of waste items. The mock-waste drum is constructed in three equally-spaced vertical sections each physically separated by a 1.3-cm-thick Plexiglas divider. The bottom section of the drum contains medium-density items that are representative of TRU waste. The middle section contains medium- to high-density items found in LLW and the upper section contains combustible, low-density materials that are representative of LLW. The mock-waste drum also includes three, 3.18-cm outside diameter, aluminum tubes that penetrate the drum from the outside top to the bottom and pass through each section including the dividers as shown in the diagram of Figure 14. The position of the three tubes within the drum is the same as that described in the first reference experiments above. More details about the construction of this mock-waste drum can be found in reference CAM94.

We performed two A&PCT scans of the mock-waste drum. The locations where the measurements were performed on the drum are shown in the diagram in Figure 14. The figure also shows the approximate locations of the radioactive source placed within the aluminum tube for each scan. The first scan was acquired at the center of the upper section of the waste drum and the second scan was acquired at the center of the middle section of the drum. The upper section of the drum contains miscellaneous gloves, plastic bottles, Kim-wipes, Q-tips, aerosol cans, CYNROC pellets, wood and expanding foam that is used to immobilize the contents. The items that were placed in the upper section of the drum are shown at the top of Figure 15. The placement of the items is shown at the bottom of Figure 15. The middle section of the waste drum contains assorted scrap metal parts, scrap aluminum, concrete, cans of Petroset, Diatomaceous earth and water, a bag of assorted tools, brackets, etc., a bag of cables, tubes, etc., and expanding foam used to immobilize the contents. The middle section items are shown at the top of Figure 16. The placement of the items is shown at the bottom of Figure 16.

A radiograph of the well characterized mock-waste drum is shown on the left of Figure 17. The figure also shows two high-spatial resolution transmission computed tomography (TCT) images on the right. These are at the approximate location where the A&PCT data was acquired. The location of the CT images are indicated by the lines drawn through the radiograph. These data were acquired by a non-destructive evaluation system, details of this measurement are given in reference MAR94.

As with the aluminum cylinder experiment, the active data was acquired using the 365-keV transition of the  $^{166m}\text{Ho}$  source and passive CT data was acquired from the 356-keV transition of the passive  $^{133}\text{Ba}$  sealed source. The passive source was inserted into the center tube position between the drum center axis and wall. The passive source had a nominal intensity of 70  $\mu\text{curies}$  at the time of the experiment that was accurately calibrated in a separate measurement. The same UCSF MLEM code used on the aluminum cylinder data was used for reconstructing the A&PCT data.

The A&PCT assay results are summarized in Figure 18 for the upper section scan of the LLW/TRU waste drum. Figure 18a is the tomogram of the ACT scan that represents an attenuation map of the waste drum contents and is used to correct the passive data for attenuation. Gross features in this attenuation map can be correlated to the higher-spatial resolution attenuation images produced by the TCT data shown in Figure 17. Figure 18b shows the passive image not corrected for attenuation at 356 keV. The tomogram shows the geometry and position of the isotope source.

Figure 18c is a reconstructed passive tomogram of the  $^{133}\text{Ba}$  source for the 356 keV energy peak corrected for attenuation using the transmission tomogram of Figure 18a. The

pixel sum of this tomogram provides a value of the peak area intensity of the radioactive source in photon counts for a 50 second integration time. This peak area intensity has been corrected for the attenuation of items that are absorbing photons between the source and the detector. The average attenuation can be determined using the corrected and uncorrected emission tomogram summed values. The sum of the corrected tomogram is listed in the table of Figure 18 and compared to the ideal (calibrated) source strength. For the low-density combustible matrix of the upper scan, the value was determined to within 2.6%.

The same analysis was performed for the middle-drum section containing the high-to-medium density matrix and is shown in Figure 19. The location of the  $^{133}\text{Ba}$  passive source is shown on the transmission image and a sum of the photon counts corrected for attenuation is shown in the table. A comparison of the measured and corrected passive source activity to the actual value is shown in the table of Figure 19. The values agree to within 5.4%.

Within the assumption of the 2D reconstruction code and the limited data sets that we have tested, we have found excellent agreement between our experimental results and the known calibration value of the emission source for these complicated attenuating matrices. Future efforts will include further tests of this method using line sources and additional sections of the mock-waste drum to better confirm these results.

## V. SUMMARY

We have found encouraging results for the application of A&PCT for the analysis of waste drums. The preliminary experiments with reference scans show that we can use the ACT data to correct the experimental PCT data for attenuation by heterogeneous-waste matrices. In our absolute assay measurements we found good agreement between our experimental results and the known calibration value of the passive source for these complicated attenuating matrices. This suggests, noting the limitations of the 2D reconstruction code, that the A&PCT can be used to produce absolute assays of radioactivity in real-waste drums.

Our future efforts will expand on these developments to further study this technology and make it applicable to real-waste drums. The development of a 3-dimensional reconstruction code will allow us to analyze radioactive sources of any geometry. We will also expand our analysis of the gamma-ray spectra to include isotope identification so that we can analyze unknown samples in an automated sample. Our plans also include the optimization of this "single-detector" technique and to study the feasibility of upgrading the system to a multi-detector system with a higher throughput.

## VI. ACKNOWLEDGEMENTS

We thank Linwood Hester and Derrill Rikard for their help in setting up the A&PCT experiments and obtaining data. We are grateful for the many helpful discussions on passive and active CT image reconstruction with Bruce Hasegawa and Keenan Brown of the University of California at San Francisco. This work was partially funded by the Office of Technology Development in DOE's Environmental Restoration and Waste Management Program and performed under the auspices of the U.S. Department of Energy by the Lawrence Livermore National Laboratory under Contract W-7405-Eng-48.

## VII. REFERENCES

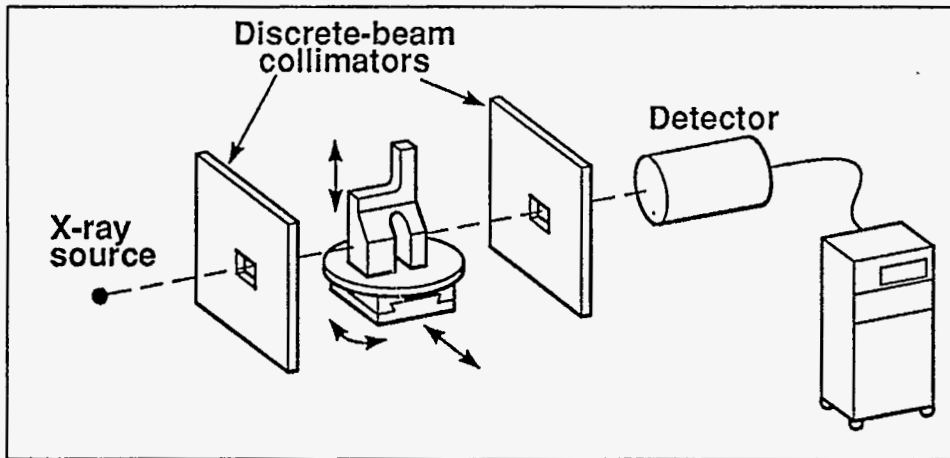
- [AND91] B. C. Anderson and D. J. Osetek, *Nondestructive Examination and Assay System Research and Development Requirements to Meet Evolving Regulations for Transuranic and Low-Level Wastes*, draft report, Waste Isolation Pilot Plant, Carlsbad, NM (1991).
- [BER94] Richard T. Bernardi and Kyung S. Han, "Nondestructive Evaluation and Assay of Nuclear Waste Drums with High Energy Transmission and Emission Computed Tomography," in *Proceedings of the Waste Management '94 Symposia*, Tucson, AZ (1994).
- [BRO92] J. K. Brown, S. M. Reilly, B. H. Hasegawa, E. L. Gingold, T. F. Lang, and S. C. Liew, "Computer simulation of an emission-transmission CT system," submitted to *Med. Phys.*
- [CAL86] J. T. Caldwell, R. D. Hastings, G. C. Herrera, W. E. Kunz, E. R. Shunk, *The Los Alamos Second-Generation System for Passive and Active Neutron Assays of Drum-Size Containers*, LA-10774-MS, Los Alamos National Laboratory, Los Alamos, NM, September 1986.
- [CAM94] David C. Camp, John Pickering, and Harry E. Martz, "Design and Construction of a 208-L Drum Containing Representative LLNL Transuranic and Low-Level Wastes," *Proceedings of the Nondestructive Assay and Nondestructive Examination Waste Characterization Conference*, Pocatello, Idaho, February 14-16, 1994; UCRL-JC-115672, Lawrence Livermore National Laboratory, Livermore, CA, February 1994.
- [CAM92] D. C. Camp and H. E. Martz, "Nondestructive Characterization of TRU and LLW Mixed-Wastes Using Active and Passive Gamma-Ray Spectrometry/Computed Tomography," *Proc. Information Exchange Meeting on Characterization, Sensors, and Monitoring Technologies*, Dallas, TX, July 15-16, 1992.
- [DEB88] K. Debretin and R. G. Helmer, Gamma- and X-Ray Spectrometry with Semiconductor Detectors, (Elsevier, New York, NY, 1988).
- [EST90] R. J. Estep, *Assay of Heterogeneous Radioactive Wastes by Low-Resolution Tomographic Gamma Scanning*, Los Alamos National Laboratory, Los Alamos, NM, LA-UR-90-2054 (1990).
- [GOT91] H. Gotoh, Japan Atomic Energy Research Institute, Tokai-Mura, Naka-Gun, Ibaraki-ken 319-11 Japan, private communication (1991).
- [HUE77] R. H. Huesman, G. T. Gullberg, W. L. Greenberg, and T. F. Budinger, *RECLBL Library Users Manual*, Lawrence Berkeley Laboratory, Berkeley, CA, Pub 214 (1977).
- [KAW90] S. Kawasaki, M. Kondo, S. Izumi, and M. Kikuchi, "Radioactivity Measurement of Drum Package Waste by a Computed-Tomography Technique," *Appl. Radiat. Isotopes* 41, 983 (1990).



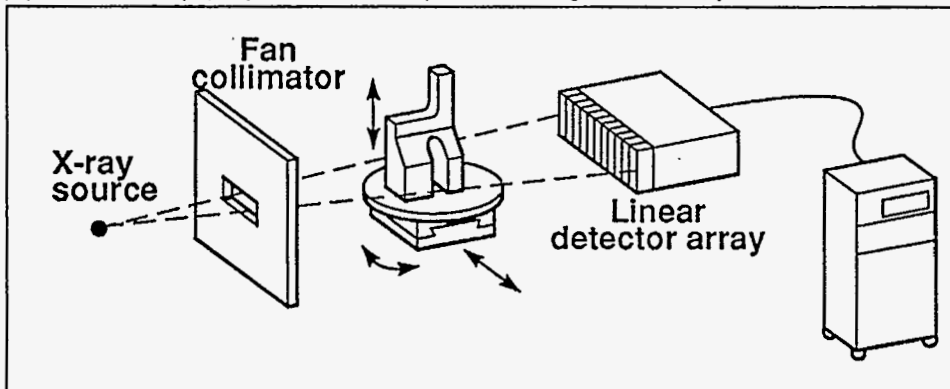
- [LEV94] F. Lévai, Institute of Nuclear Techniques, Technical University of Budapest, H-1521 Budapest, Hungary, private communication (1994).
- [MAR94] H. E. Martz, D. J. Schneberk, and G.P. Roberson, "Real-Time Radiography, Digital Radiography, and Computed Tomography for Non intrusive Waste Drum Characterization," *Proceedings of the Nondestructive Assay and Nondestructive Examination Waste Characterization Conference*, Pocatello, Idaho, February 14-16, 1994; UCRL-JC-115670, Lawrence Livermore National Laboratory, Livermore, CA, February 1994.
- [MAR91] H. E. Martz, S. G. Azevedo, G. P. Roberson, D. J. Schneberk, Z. M. Koenig, and D. C. Camp, "Considerations for an Active and Passive CT Scanner to Assay Nuclear Waste Drums," in *ASNT's 1991 Industrial Computed Tomography II Topical Conference, Paper Summaries*, May 20-24, San Diego, CA (1991), p. 143.
- [MAR90] H. E. Martz, G. P. Roberson, D. J. Schneberk, M. F. Skeate, D. Perkins, and S. G. Azevedo, *Computed Tomography of a Simulated Waste Canister*, Lawrence Livermore National Laboratory, Livermore, Calif., UCID-21940 (1990).
- [MAR92] H. E. Martz, G. P. Roberson, C. Robert-Coutant, D. J. Schneberk, and D. C. Camp, *Quantitative Waste-Form Assay Using Gamma-ray Computed Tomography*, Lawrence Livermore National Laboratory, Livermore, CA, UCRL-JC-110648 (1992); *Proc. Int. Symp. Spectrosc. and Struct. Molec. Nuclei*, March 27-29, 1992, Tallahassee, FL.
- [MAR92a] H. E. Martz, D. J. Schneberk, G. P. Roberson, and S. G. Azevedo, *Computerized Tomography*, Lawrence Livermore National Laboratory, Livermore, CA, UCRL-53868-91 (1992).
- [MAR92b] H. E. Martz, G. P. Roberson, C. Robert-Coutant, D. J. Schneberk, and D. C. Camp, "Quantitative Waste Assay Using Gamma-Ray Spectrometry and Computed Tomography," in *Proc. 14th Annual ESARDA Meeting*, Salamanca, Spain, May 4-8, 1992, p. 273.
- [MAR92c] H. E. Martz, G. P. Roberson, C. Robert-Coutant, and D. C. Camp, "Experimental A&PCT Research and Development Efforts to Characterize Mixed Waste Forms," , *Proceedings of the Transuranic Waste Characterization Conference*, Idaho State University, Pocatello, Idaho, August 10-12, 1992; UCRL-JC-110826, Lawrence Livermore National Laboratory, Livermore, CA, December, 1992.
- [REI92] P. Reimers, "Quality Assurance of Radioactive Waste Packages by Computerized Tomography, Task 3, Characterization of Radioactive Waste Forms; A Series of Final Reports (1985-89) - No. 37," *Nuclear Science and Technology*, EUR 13879 EN, Commission of the European Communities, Luxembourg, 1992.

- [ROB92] C. Robert-Coutant, H. E. Martz, and S. G. Azevedo, "Simulated A&PCT Data to Study the Mixed Waste Forms Characterization Problem," *Proceedings of the Transuranic Waste Characterization Conference*, Idaho State University, Pocatello, Idaho, August 10-12, 1992
- [SIM90] S. M. Simmonds, J. K. Sprinkle, Jr., S.-T. Hsue, and M. P. Kellogg, *Nondestructive Assay of Plutonium Bearing Scrap and Waste with the Advanced Segmented Gamma-Ray Scanner*, LA-UR-90-2253, Los Alamos National Laboratory, Los Alamos, NM, 1990.

(a) Single discrete detector (1st generation, parallel beam)



(b) Linear-array (1D) of detectors (2nd or 3rd generation, parallel or fan beam)



(c) Area-array (2D) of detectors (2nd or 3rd generation, parallel or cone beam)

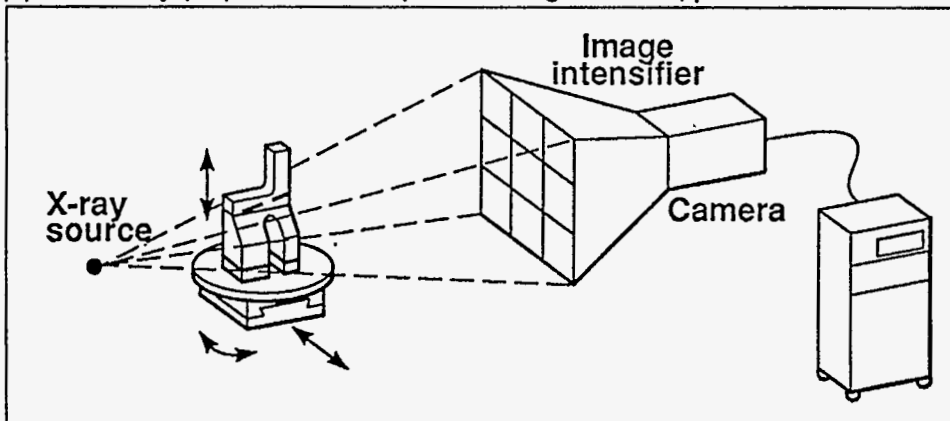


Figure 1 CT data-acquisition geometries of computed tomography scanners: (a) Single, nuclear-spectroscopy detector, discrete-beam translate/rotate design, (b) well-collimated fan-beam design using a linear detector array, and (c) cone-beam design using an area-array (2D) detector.

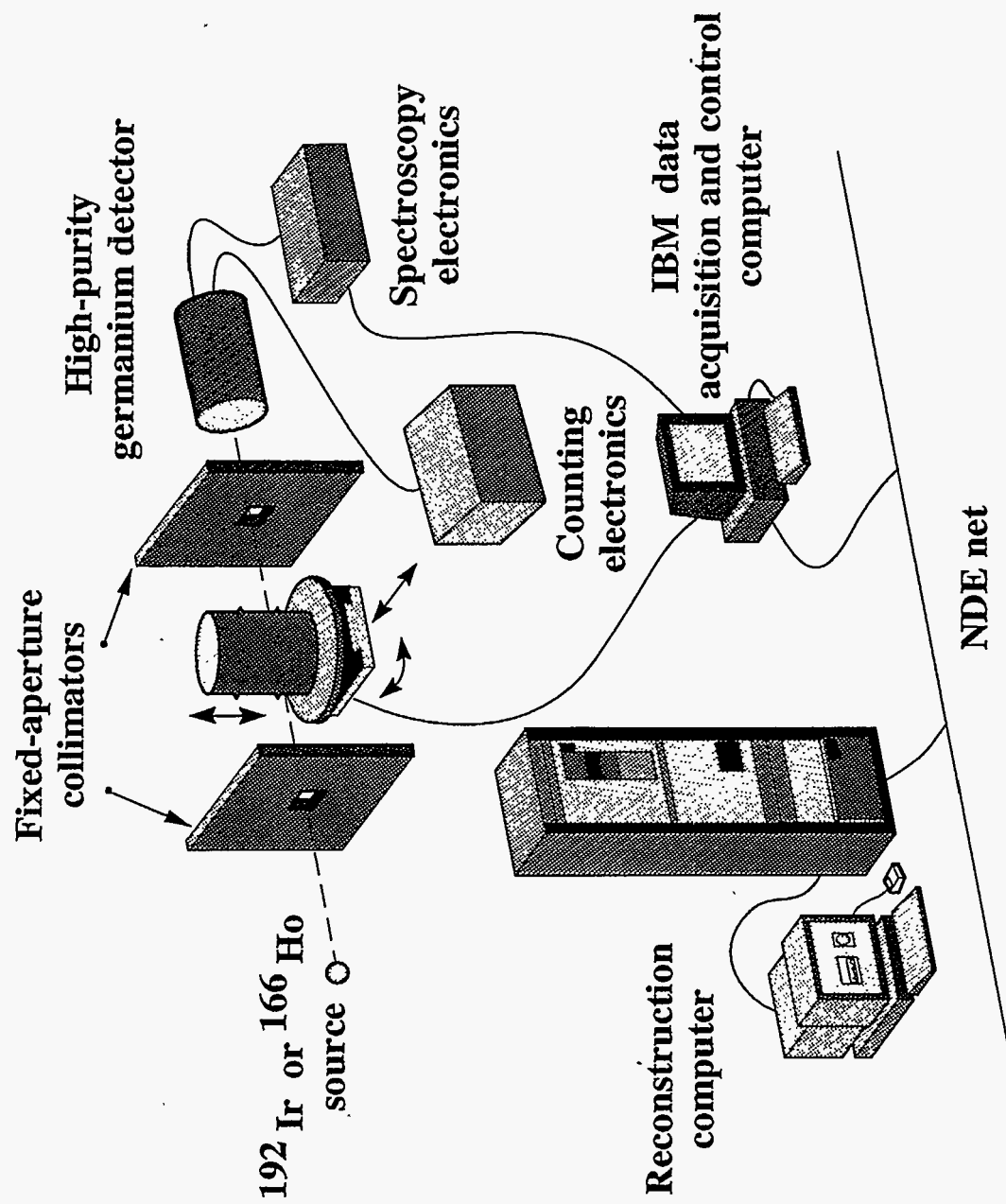


Figure 2

The block diagram displays the major components that are required for the prototype A&PCT system including: a transmission source, source and detector collimators, 3-axis drum manipulator, HPGe detector and spectroscopy electronics, data acquisition and control computer, and image reconstruction computer.



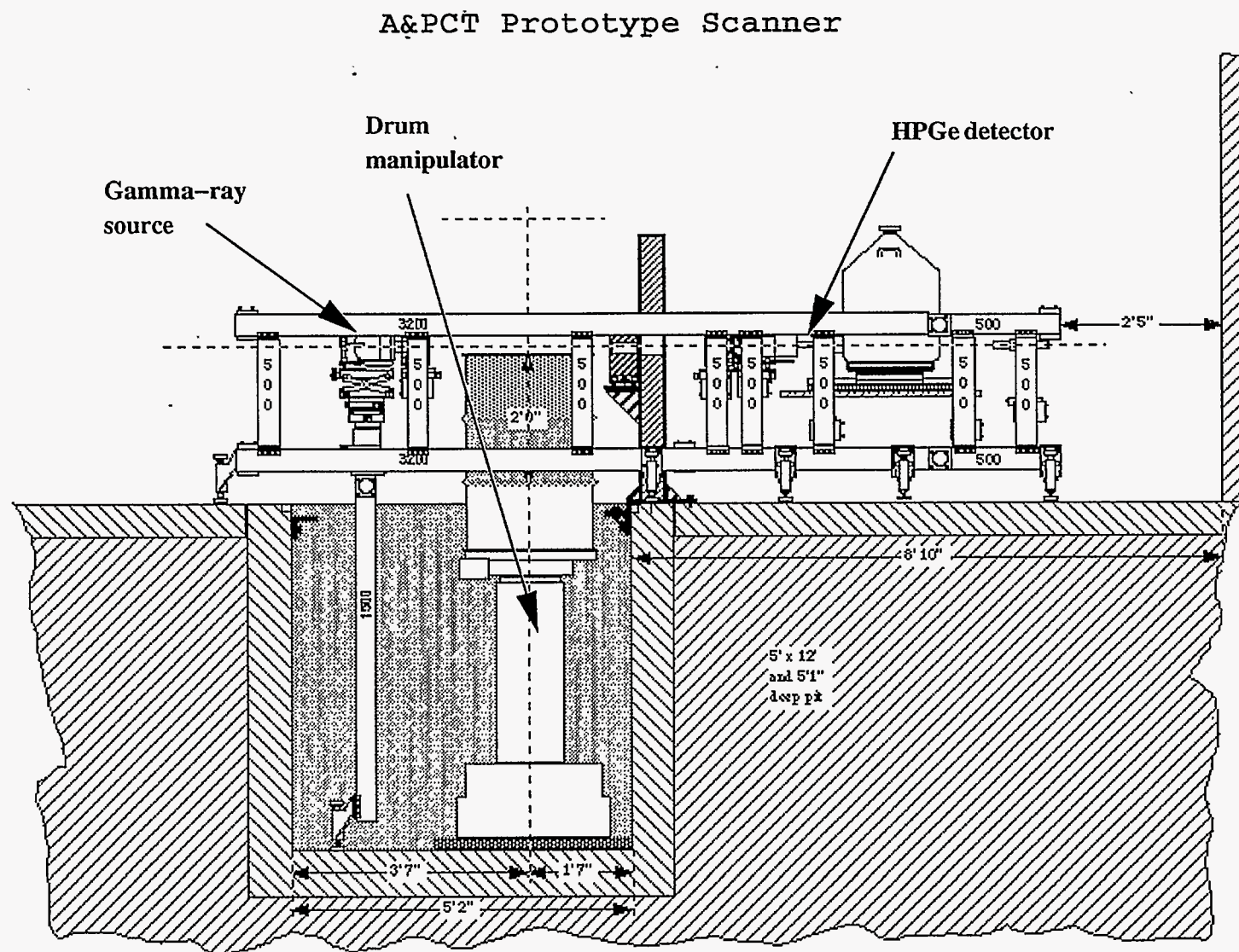


Figure 3 Engineering drawing of the prototype A&PCT system showing the placement of the major components. The drum manipulator resides in a pit in the floor, this allows the other system components to remain low to the ground.

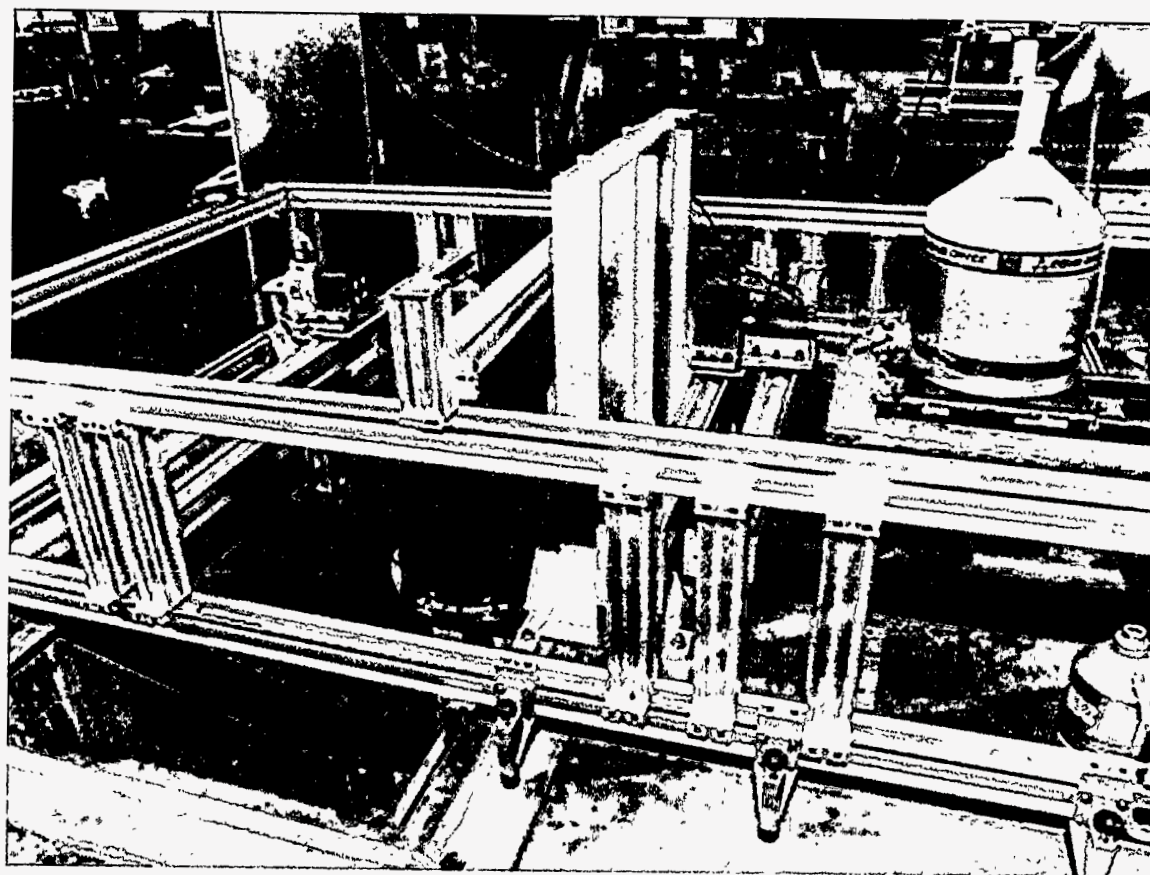


Figure 4 A photograph of the prototype A&PCT system that resides at Livermore's Site-300. Starting at the left of the photograph, the source and associated collimator supported by the system frame, the drum manipulator in the building pit, the heavy lead wall and the detector and associated collimator also supported by the system framework. The system framework is made of clamping rails that provide the flexibility to reconfigure the system for different experiments.

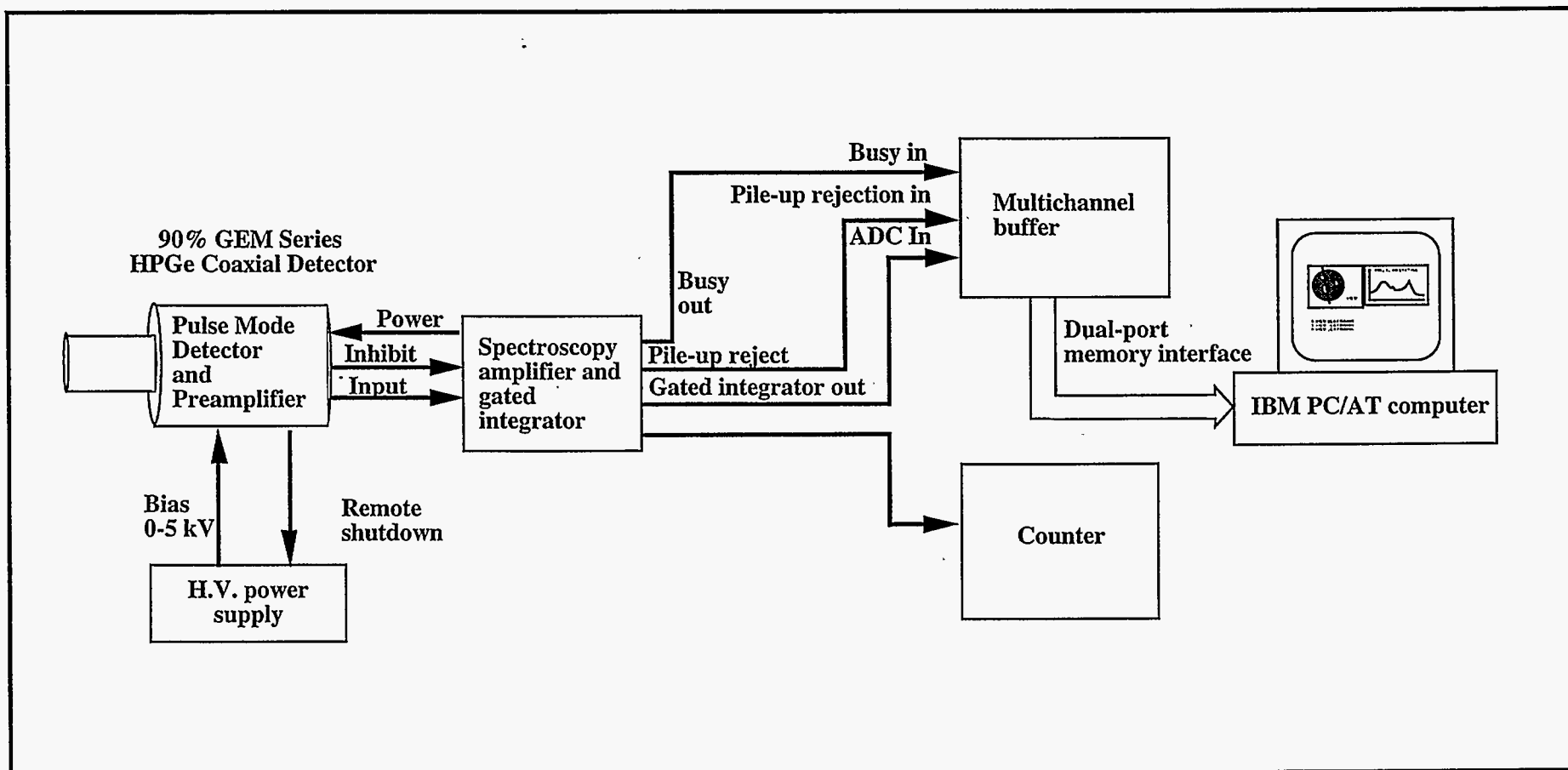


Figure 5 Representative schematic of the A&PCT scanner's nuclear-spectroscopy-based electronics showing the detector and all downstream electronic components. The incoming photons are detected by a high-purity germanium detector, preamplifier (part of the detector), then amplified. The amplified signal is sent to a multichannel analyzer (MCA) and digitized. The output from the MCA is sent to a PC for storage and preprocessing. The signal from the amplifier is also sent to a counter/timer module for real time observation of the activity of the gamma-ray sources.

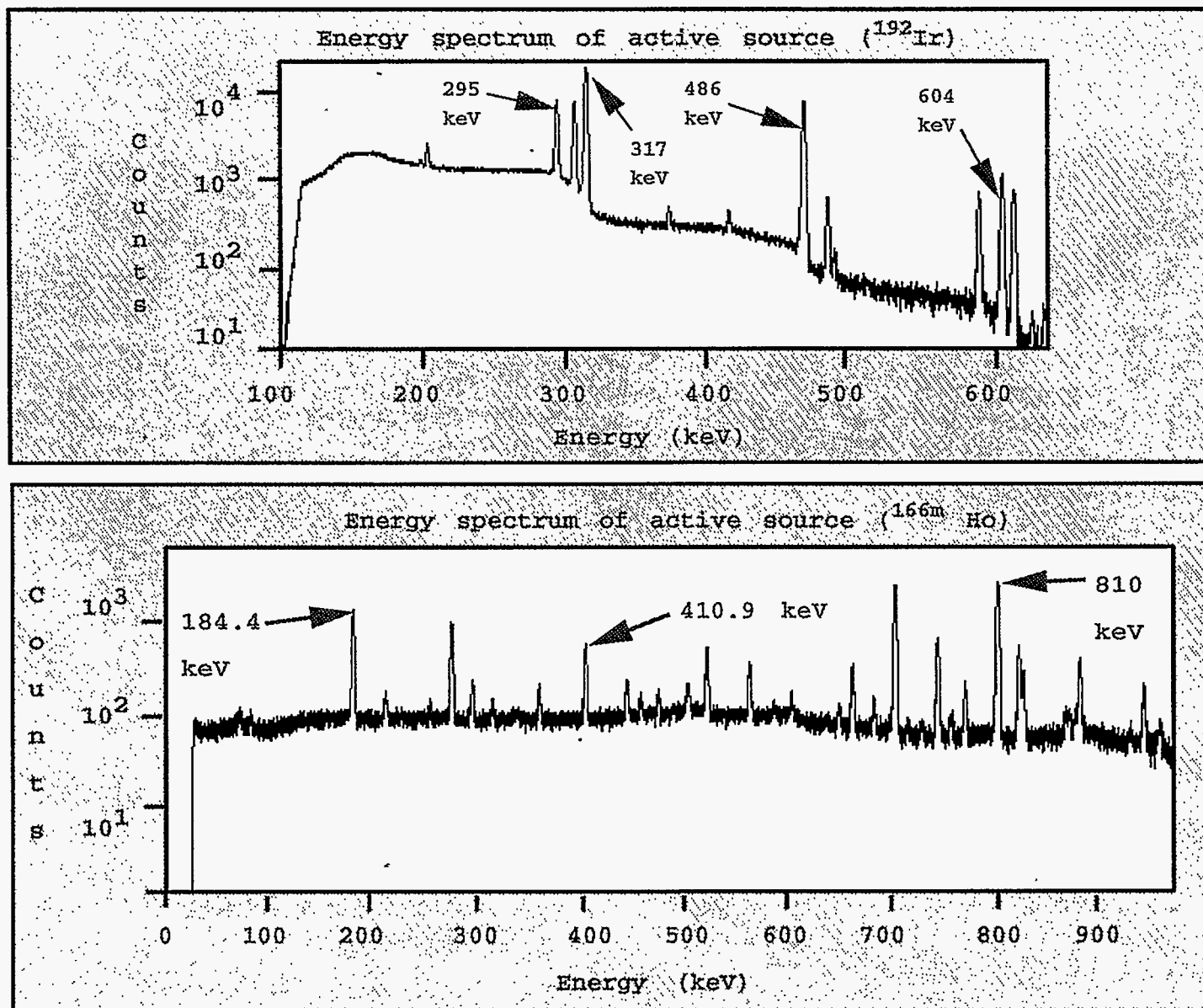
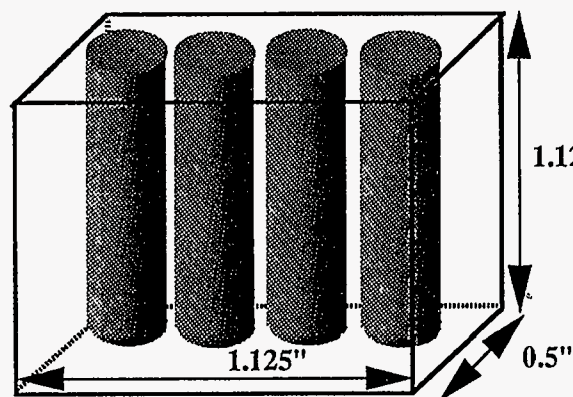
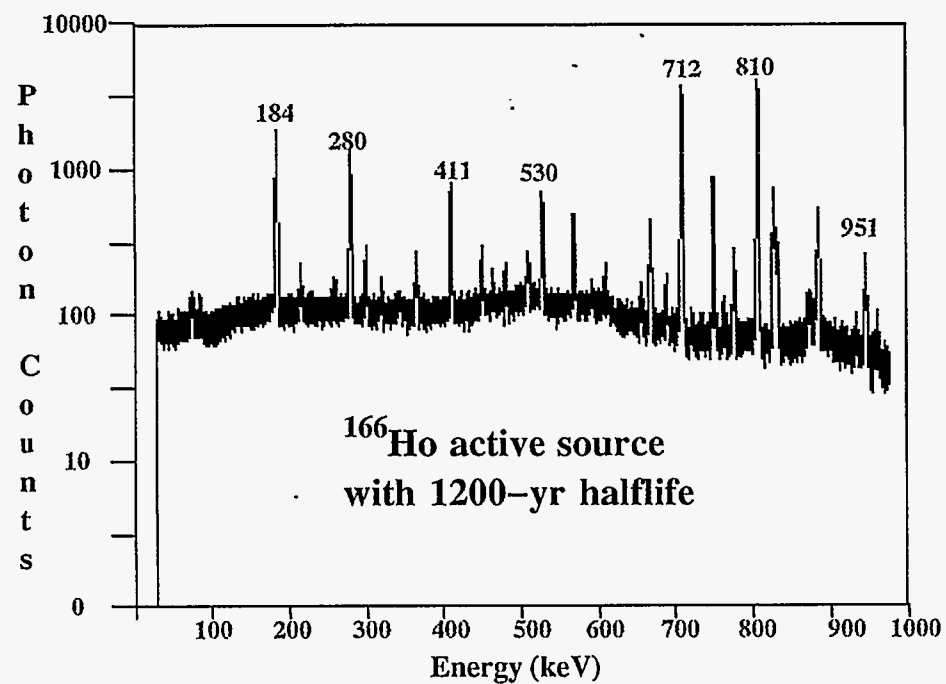


Figure 6 Attenuated spectra from two different active sources with major peaks or branches identified. The two sources that have been used are  $^{192}\text{Ir}$  (top) and  $^{166\text{m}}\text{Ho}$  mixed with  $^{60}\text{Co}$  (bottom).





Each cube has  
approximately  
1.4 mCi of  $^{166}\text{Ho}$   
and 0.2 mCi of  $^{60}\text{Co}$

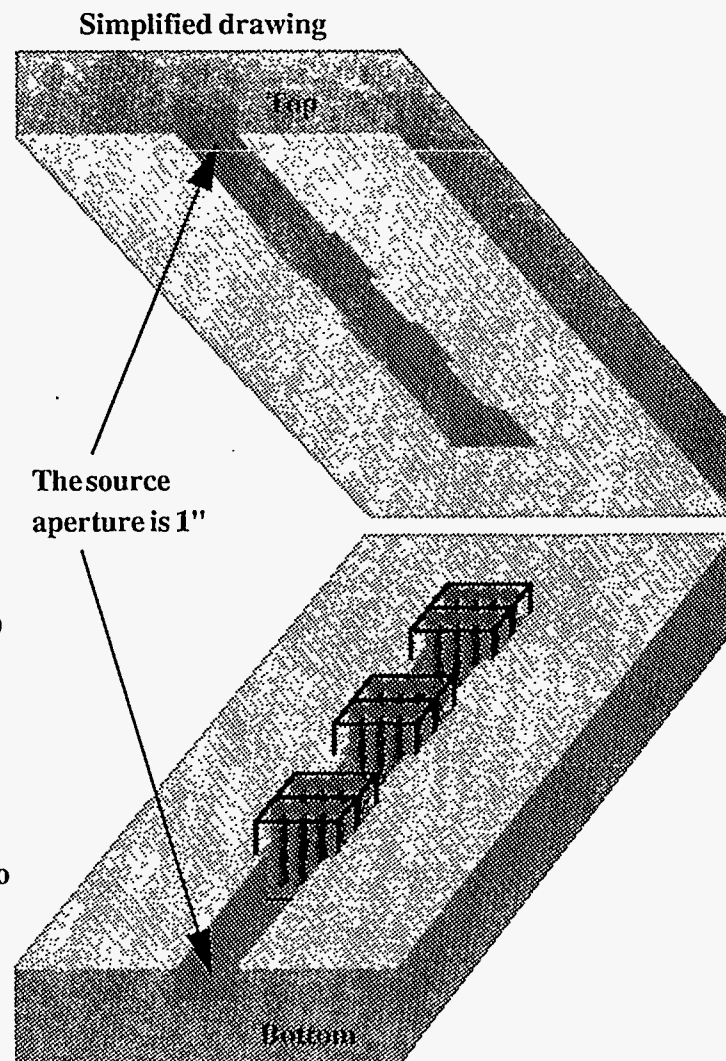


Figure 7 A diagram of the Lucite  $^{166}\text{mHo}$  source holder is shown to the lower left. Eight individual capsules were loaded into each Lucite holder. Two capsules were placed into each of the four holes, one on top of the other. Six such cubes are held in the specially made Pb source holder shown at the right of the figure. A spectrum of the  $^{166}\text{mHo}$  source is shown at the upper left.

The aspect ratio of the A&PCT prototype scanner can be adjusted by moving the detector assembly towards or away from the lead wall

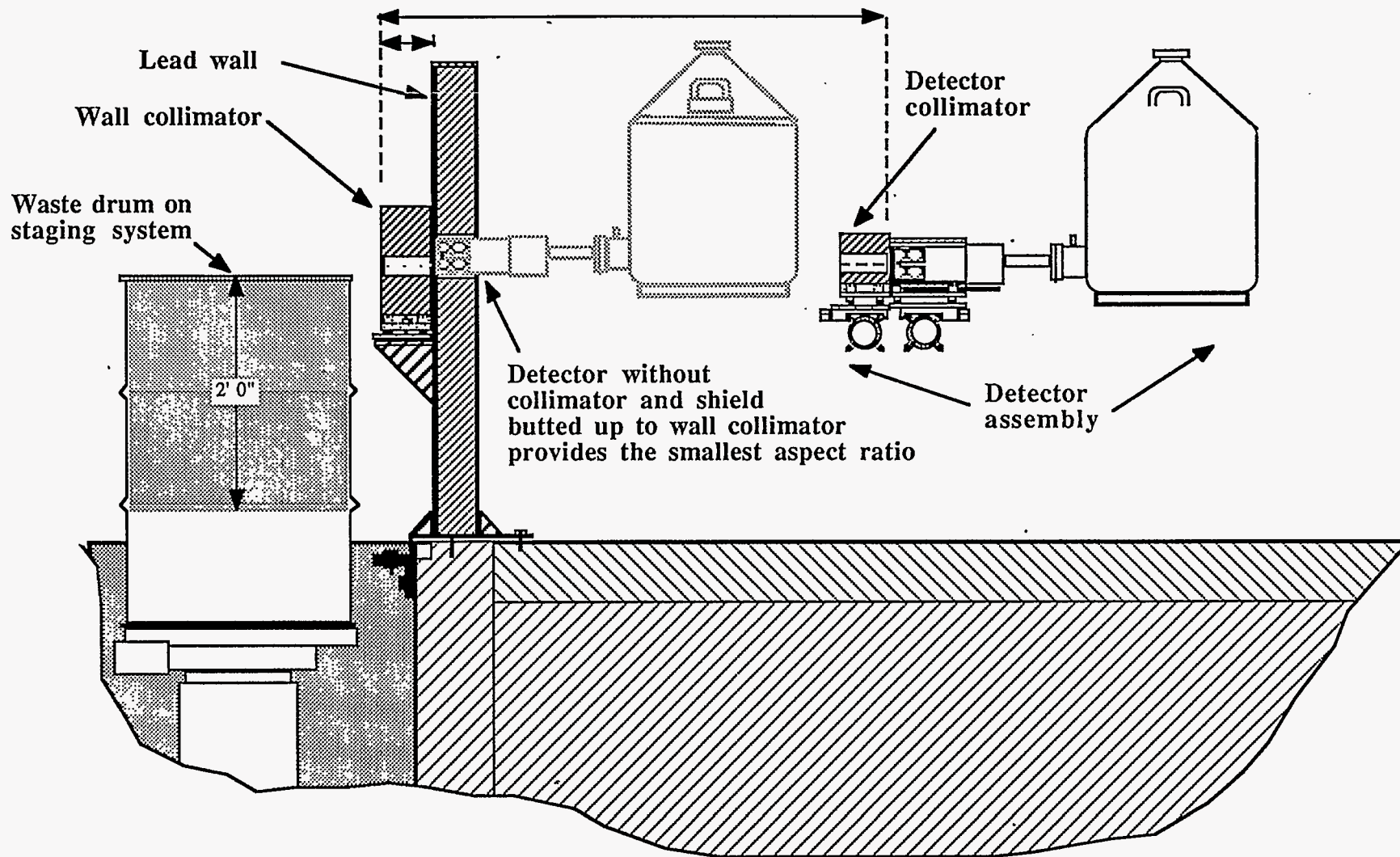


Figure 8 The aspect ratio of the A&PCT prototype scanner is adjusted by moving the detector and its associated collimator towards or away from the lead wall shown in the figure. The detector collimator and shielding can be removed from the system frame and the detector can be inserted into the lead wall to achieve the smallest possible aspect ratio.

## Mock waste drum schematic

## Computed tomography schematic

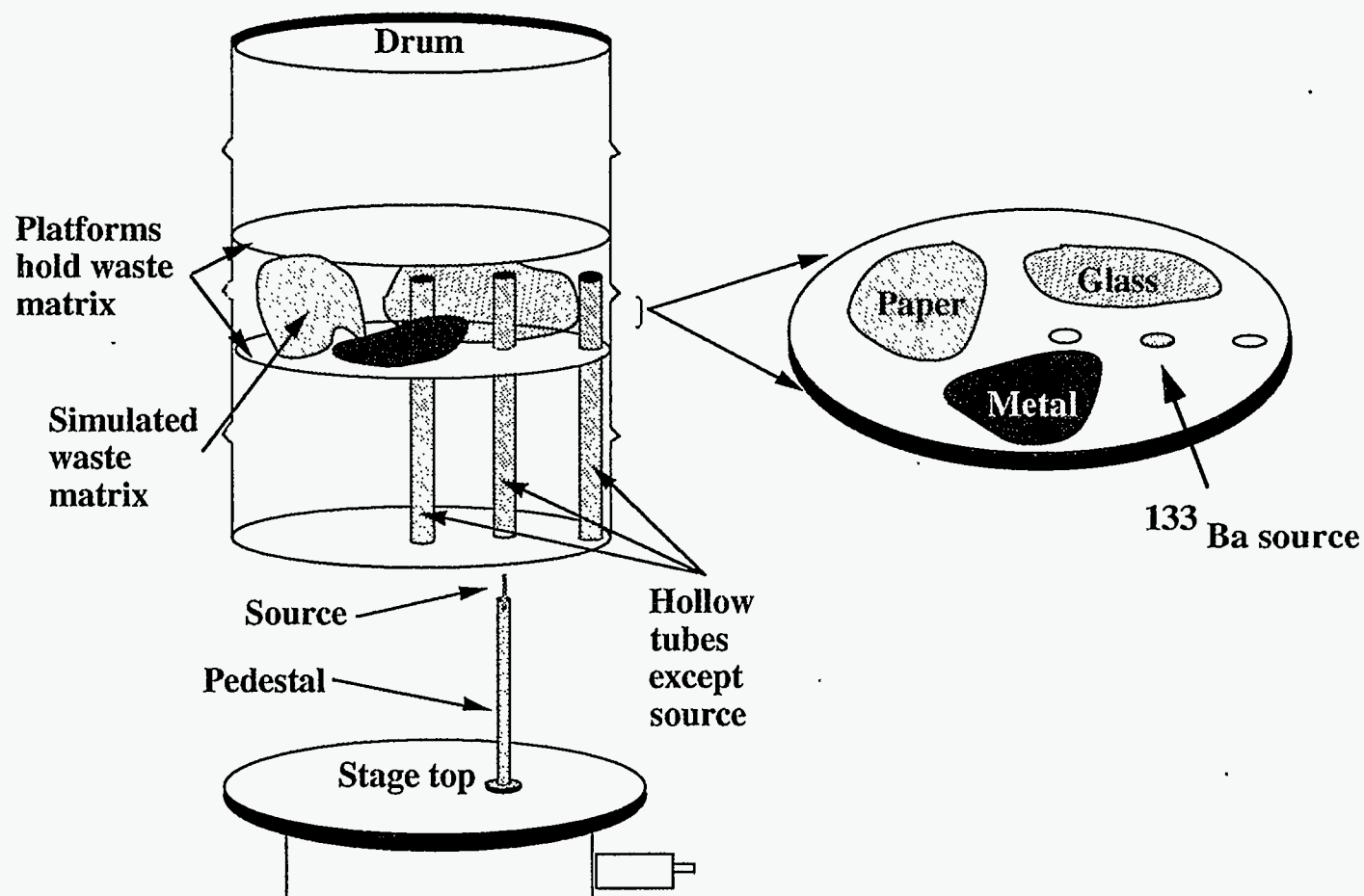
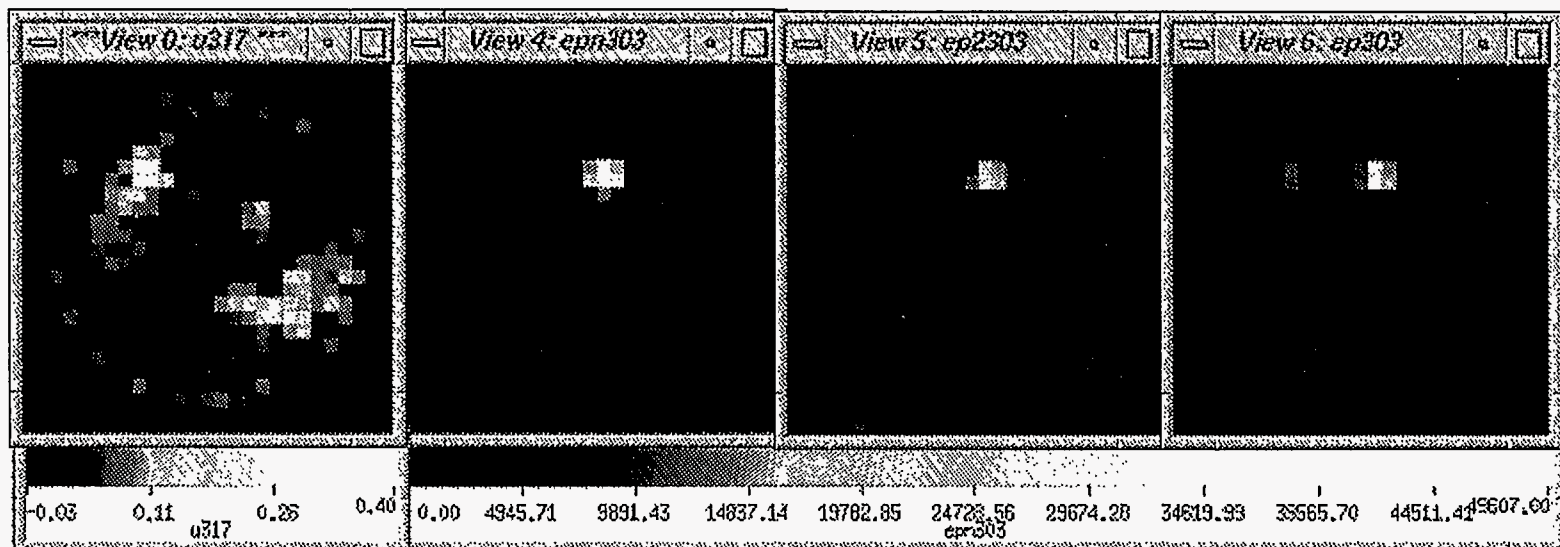


Figure 9 The waste drum was constructed with a shelf in the center to hold the simulated waste matrix of paper, glass and metal. There are three tubes that penetrate the drum into which the passive source and pedestal are inserted. The source and pedestal are fastened to the rotary stage top and can be scanned with and without the drum and waste matrix present. The diagram on the right of the figure shows where the A&PCT scans were taken.

# 150 second integration time



(a) Active CT image

(b) Reference image  
254 x 10<sup>3</sup> counts

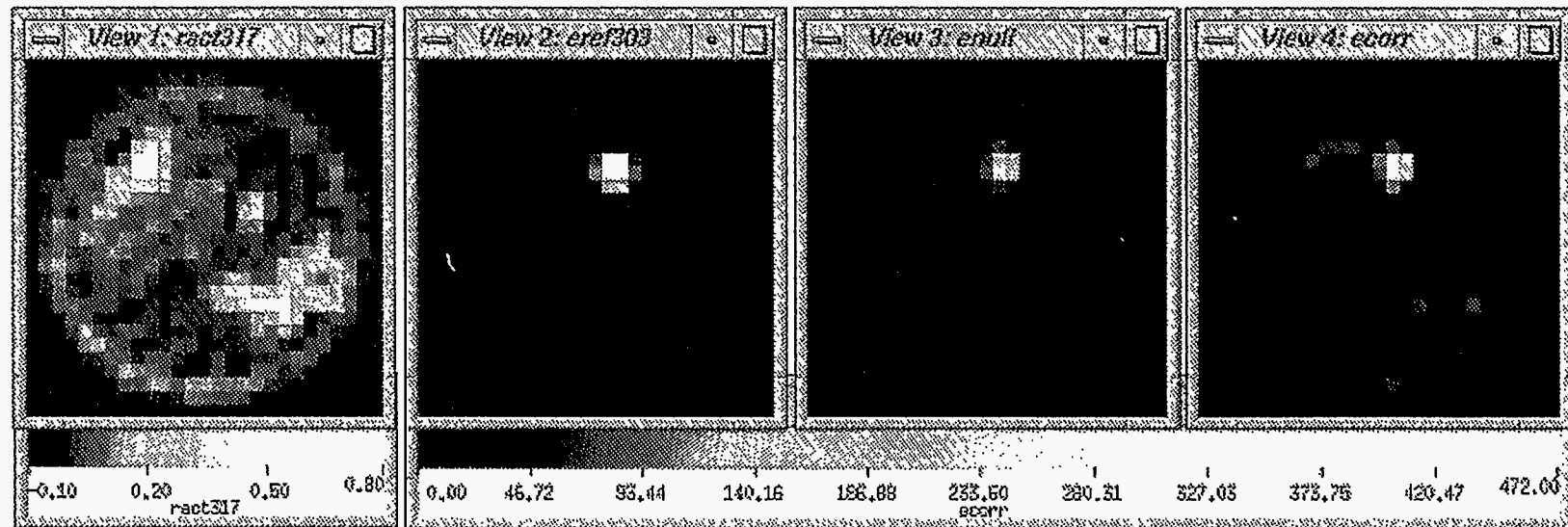
(c) Uncorrected passive  
141 x 10<sup>3</sup> counts

(d) Corrected passive  
279 x 10<sup>3</sup> counts

Figure 10: Representative reconstructed ACT (a) and PCT (b-d) images of the full size 208-liter simulated waste drum for the 150 second integration time. For the ACT image, the colorbar (a, bottom) provides a scale relating the different gray shades in the CT image to the linear attenuation coefficient in  $\text{cm}^{-1}$ . The attenuation variations are related to changes in *density* ( $\rho$ ) and/or *effective-atomic number* ( $Z_{\text{eff}}$ ). For the PCT images, the colorbar represent the photon counts accumulated at each pixel during the integration period. The summed counts are shown at the bottom for each PCT image



1.5 second integration time



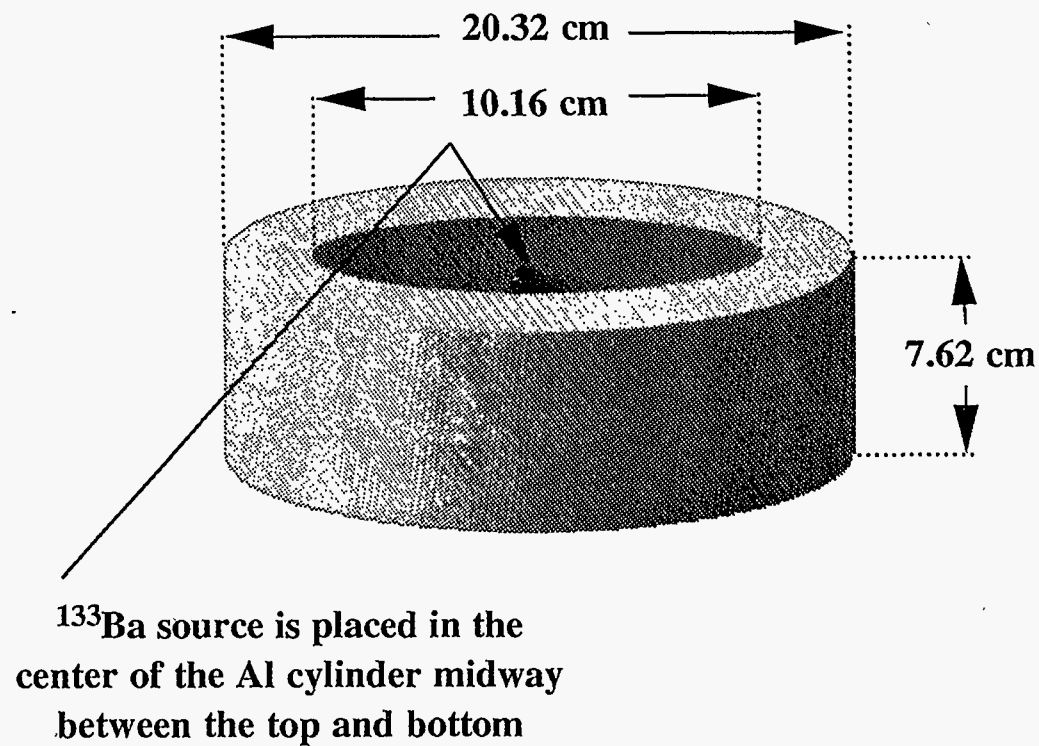
(a) Active CT image

(b) Reference image  
 $2.75 \times 10^3$  counts

(c) Uncorrected passive  
 $1.56 \times 10^3$  counts

(d) Corrected passive  
 $3.03 \times 10^3$  counts

Figure 11: Representative reconstructed ACT (a) and PCT (b-d) images of the full size waste drum for the 1.5 second integration time.



### Aluminum cylinder used for uniform attenuation of emission source

Figure 12 Diagram of the aluminum cylinder used for the uniform attenuation experiments. The dimensions of the cylinder are labeled on the figure and the placement of the passive source is shown.

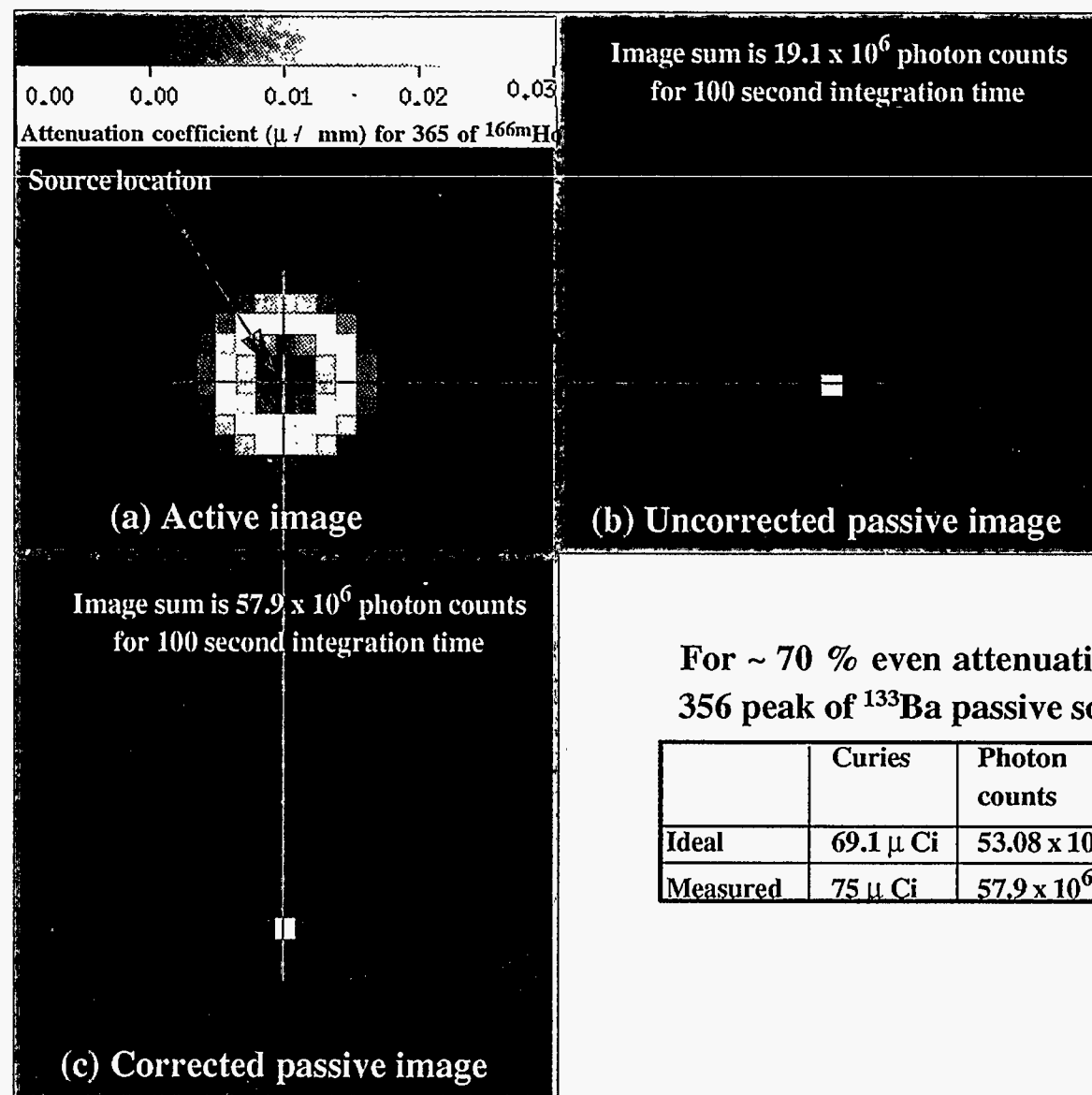


Figure 13 Representative reconstructed ACT (a) and PCT (b & c) images of the aluminum cylinder used to study a uniformly attenuated data set. For the ACT image, the colorbar is shown at the top of the active image. The results of this experiment are summarized in the table shown in the figure.

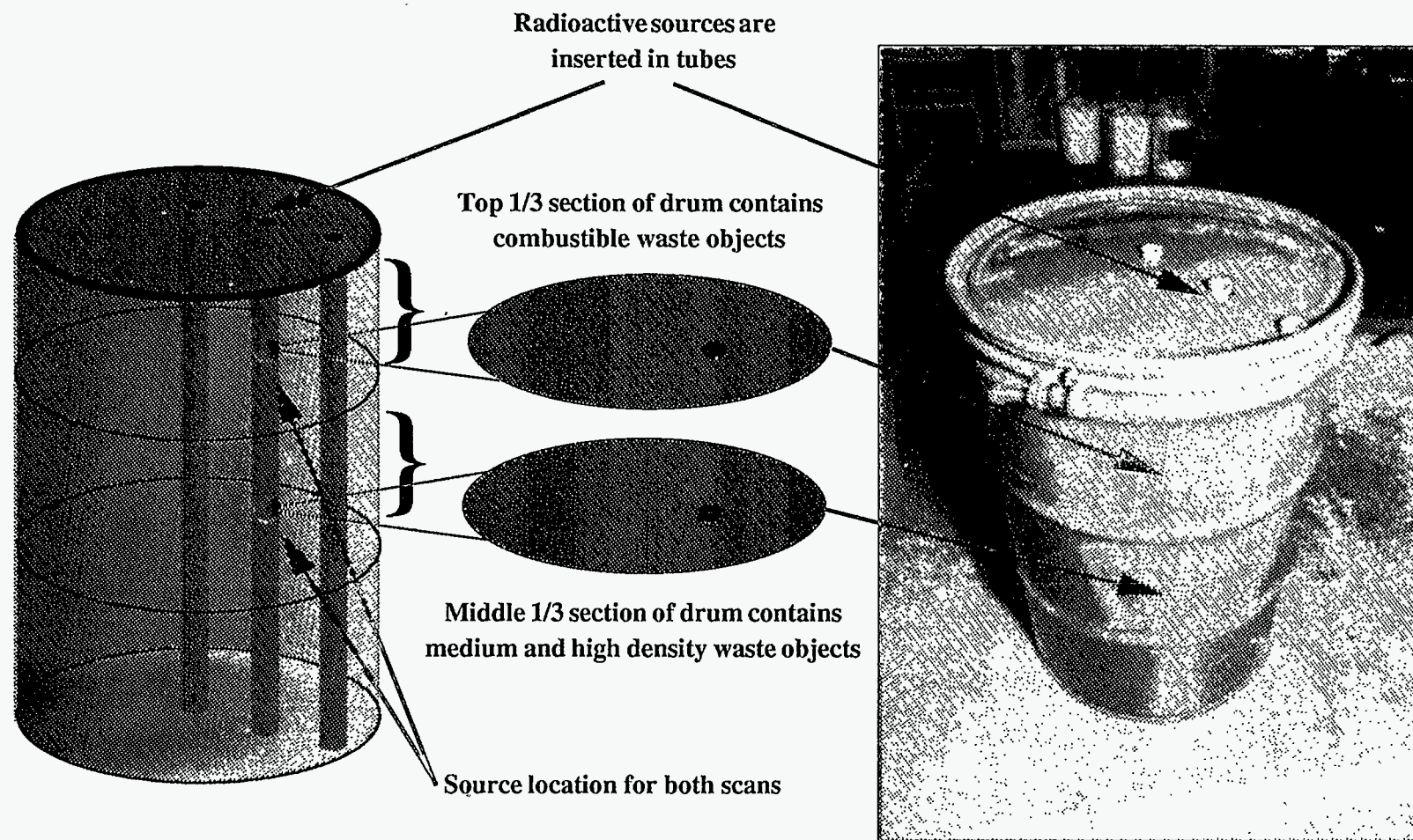
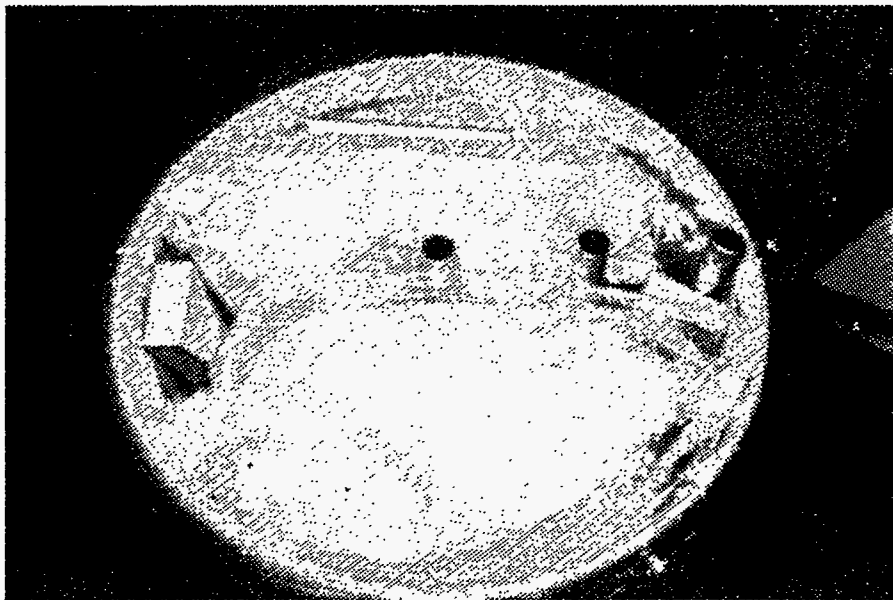
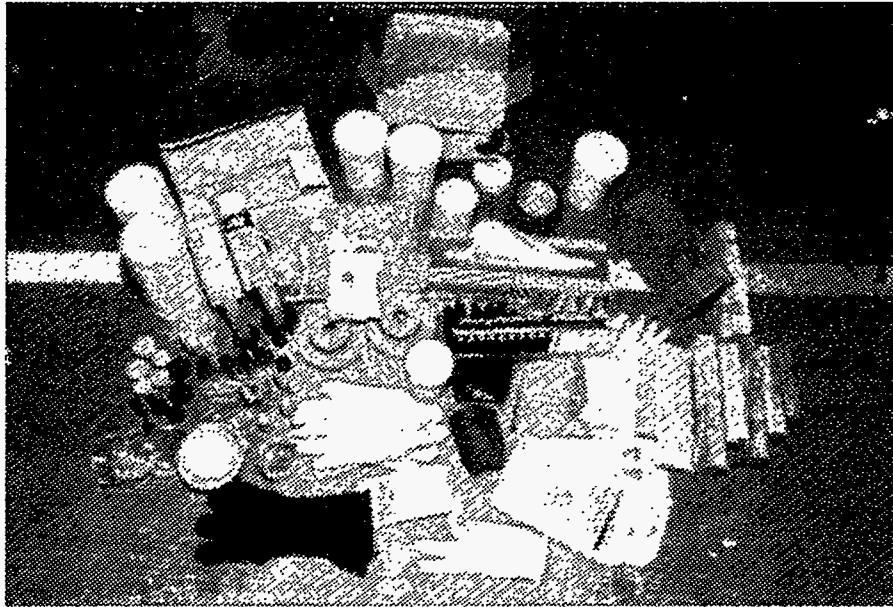


Figure 14 Diagram (left) and photograph (right) of the well characterized mock-waste drum containing representative low-level waste (LLW) and transuranic (TRU) waste items. The locations of the two A&PCT scans acquired are shown in the figure.



**Top section contains combustible low density waste matrix**

Figure 15 The top section of the mock-waste drum was loaded with a low-density waste matrix. The materials that were placed in the upper section of the drum are shown in the top of the figure. The placement of these materials are shown at the bottom of the figure.



## Middle section contains high and medium density waste matrix

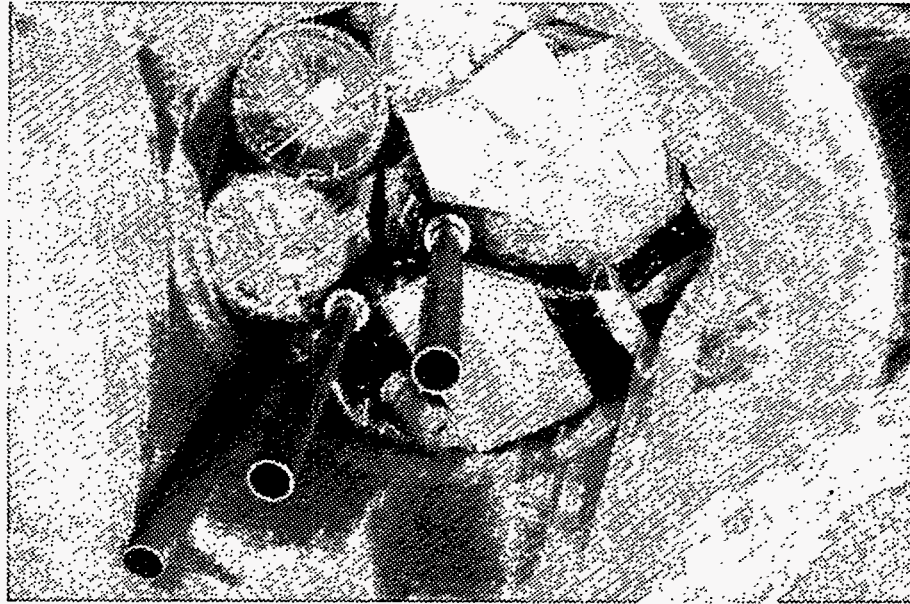


Figure 16 The middle section of the mock-waste drum contains a medium-density waste matrix. The materials used in the middle section are shown at the top and the placement of these objects is shown at the bottom of the figure.

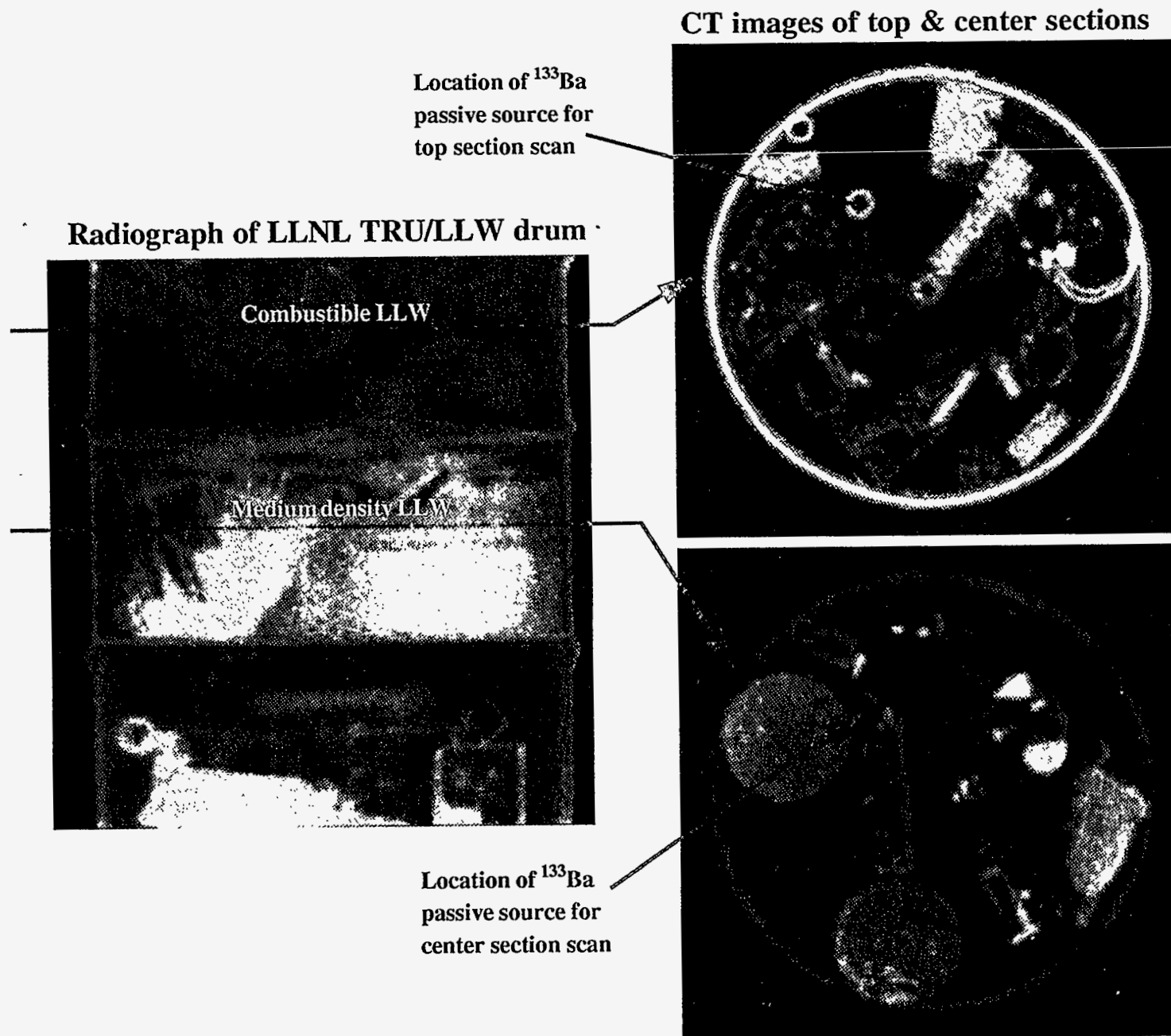


Figure 17 A digital radiograph of the well characterized mock-waste drum is shown to the left of the figure and two high spatial resolution TCT scans are shown to the right. The TCT scans shown here were both taken in the same approximate location as the A&PCT data was acquired.

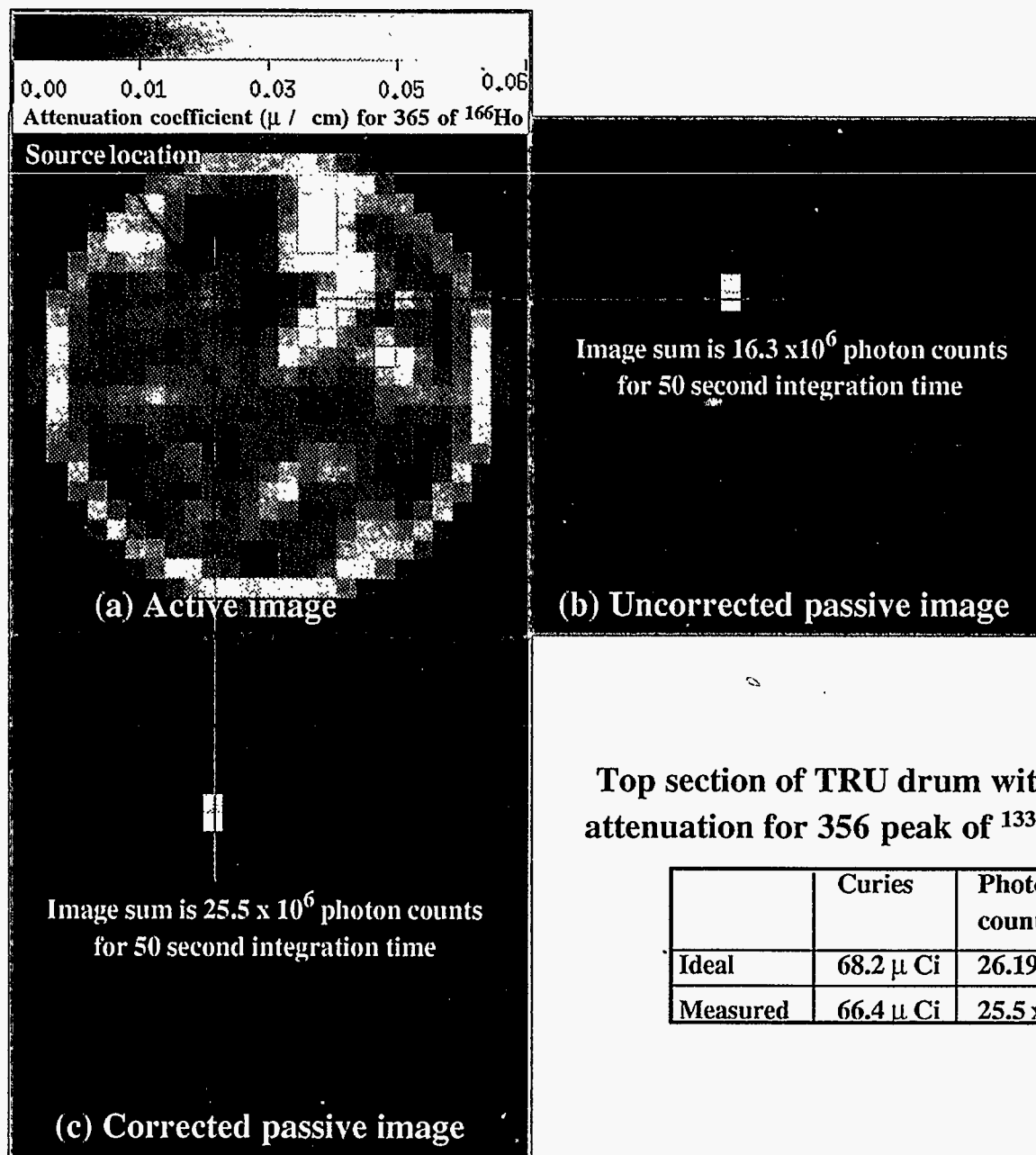


Figure 18 Representative reconstructed ACT (a) and PCT (b & c) images of the top section of the well characterized mock-waste drum. For the ACT image, the colorbar is shown at the top of the active image and the results of this experiment are summarized in the table shown in the figure.



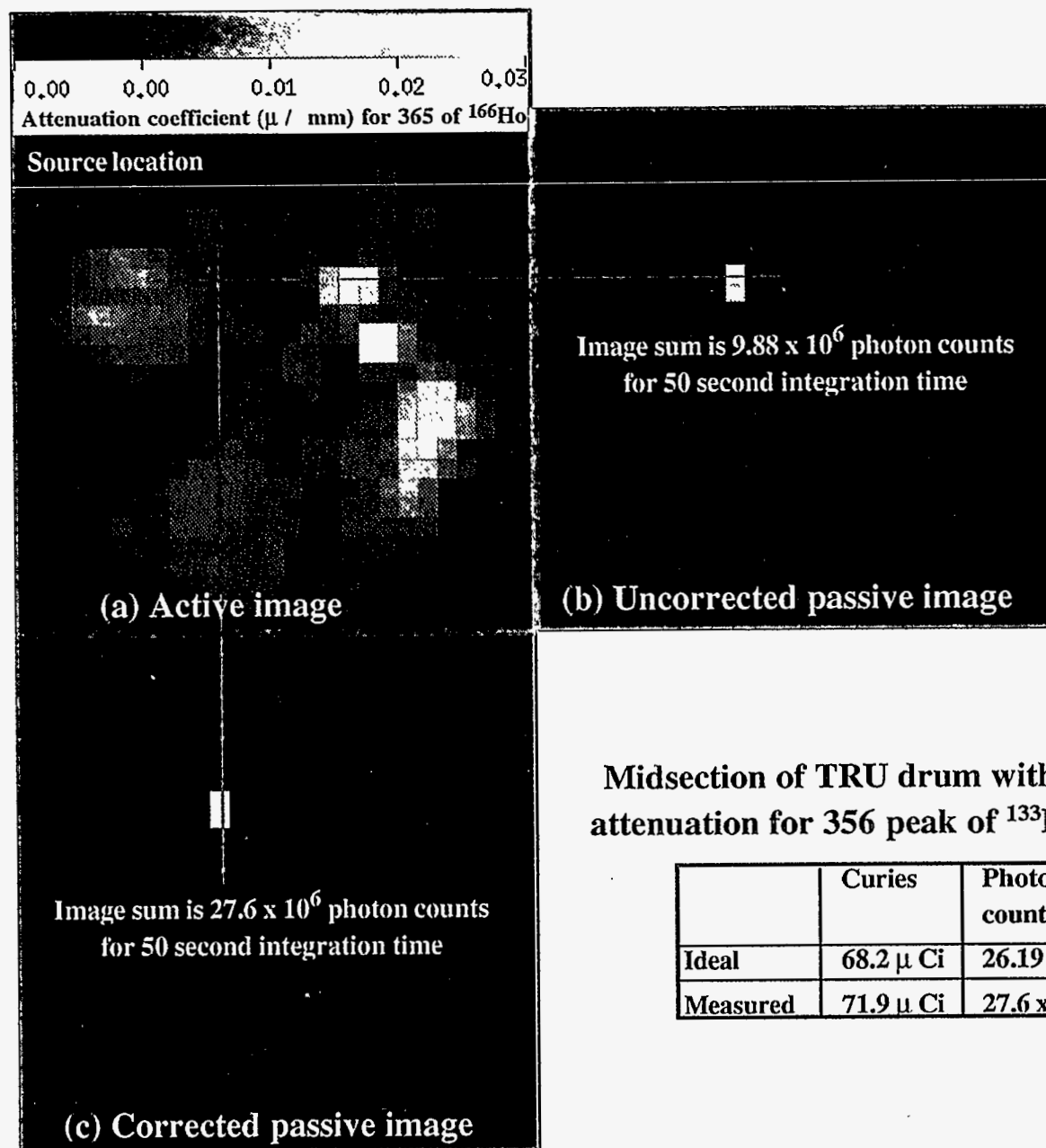


Figure 19 Representative reconstructed ACT (a) and PCT (b & c) images of the mid-section of the well characterized mock-waste drum. The results of this experiment are summarized in the table shown in the figure.